An Ecosystem Model for the Simulation of Physical and Biological Oceanic Processes—IDAPAK User's Guide and Applications

Charles R. McClain, NASA Goddard Space Flight Center, Code 970.2, Greenbelt, Maryland

Sergio R. Signorini, SAIC General Sciences Corporation, Laurel, Maryland

King-Sheng Tai, SAIC General Sciences Corporation, Laurel, Maryland

Kevin Arrigo, NASA Goddard Space Flight Center, Code 971, Greenbelt, Maryland

Ragu Murtugudde, University of Maryland, College Park, Maryland

April 1998

Contents

Prologue

Recent concern about increased levels of atmospheric CO_2 and global warming have led to studies of the ocean's role in the global carbon budget, e.g., the Joint Global Ocean Flux Study (JGOFS), and increased interest in interannual and interdecadal oceanic variability (Ocean Studies Board, [1994]; Subcommittee on Global Change Research, [1995]). Examination of historical data for these purposes is difficult because of the paucity of comprehensive time series data of sufficient accuracy and duration. For meteorological and hydrographic data, the ocean weather stations (OWS) and the Comprehensive Ocean-Atmosphere Data Set (COADS) [Woodruff et al., 1987] provide high-quality meteorological observations, and at some OWS sites, hydrographic time series are available. However, long time series of biological quantities, e.g., profiles of chlorophyll a and column-integrated primary productivity, are relatively scarce, and only recently have comprehensive time series been initiated at Hawaii and Bermuda (Karl and Michaels [1996]). Alternatively, investigations of the impact of long-term changes in meteorological forcing on ocean physics and biology can be pursued using coupled models of physical and biological processes.

Two contrasting oceanic study areas are addressed in this technical memorandum (TM): the Pacific Warm Pool and OWS P ($50°N$, $145°N$). The two areas are different in almost every aspect including seasonality, interannual variability, surface flow, and mixed layer dynamics. At OWS P, there is a distinct seasonal cycle in all physical and biological parameters, the flow is not well organized and relatively weak, vertical mixing is predominantly governed by convective processes, and local physical processes are dominant. In contrast, in the Warm Pool region the seasonal cycle is practically absent with interannual signatures (e.g., the El Niño Southern Oscillation, ENSO, and remote forcing) being the major contributing factor in the physical and biological variability. The flow is very swift and is characterized by the large-scale equatorial current system which extends across the entire tropical Pacific. Because of the presence of the Equatorial Undercurrent, the vertical changes in velocity are quite intense, and therefore, vertical mixing is predominantly controlled by the vertical shear. Also, OWS P is ideal for studying the effects of meteorological forcing [Denman and Miyake, 1973; Large et al., 1994] because it is subject to a large seasonal temperature (heat flux) cycle and is horizontally uniform with minimal horizontal advection. The climatological Ekman upwelling is positive but small because OWS P is located near the climatological transition between positive and negative wind stress curl [Reinecker and Ehret, 1988]. Thus, most of the vertical fluxes of heat and nutrients are driven by mechanical mixing and buoyancy effects. One important conclusion of Martin [1985] was that knowledge of the optical properties that control the vertical distribution of light absorption is key to understanding the behavior of the mixed layer and in estimating the performance of mixed layer models. For OWS P the optical properties are controlled by biological processes and are classified by Mueller and Lang [1989].

The Pacific Warm Pool is of particular interest because of its role in heat and moisture fluxes between the ocean and the atmosphere and, consequently, El Niño and the Southern Oscillation. It was, therefore, the site of a special experiment, the Tropical Ocean Global Atmosphere-Coupled Ocean Atmosphere Response Experiment, TOGA-COARE, from November 1992 through February 1993 [Webster and Lukas, 1992]. The longest available time series of observations for equatorial regions are at $165°E$, e.g., Delcroix and Henin [1991] and McPhaden and Hayes [1991]. As part of the Pacific Warm Pool, it is characterized by some of the warmest sea surface temperatures (SSTs) and a constant shallow mixed layer (40-50 meters) distinctly separate from the thermocline as a result of its low salinity (Lukas and Lindstrom [1991]) which presents a barrier to vertical mixing. The data have been extensively analyzed to study the SST variability [McPhaden and Hayes, 1991], heat balance [Cronin and McPhaden, 1997], and other ENSO related processes (Delcroix et al., [1992]; Delcroix et al. [1993]). Generally, heat budget and circulation studies focus on the surface fluxes, but, as noted by Lewis et al. [1990] and Siegel et al. [1995], variations in the amount of radiance penetrating through the mixed layer due to phytoplankton absorption can influence the heat budget at a significant level. This is particularly true of the Warm Pool where relatively small changes in SST and mixed layer heat content can stimulate a substantial response in large scale weather patterns.

To address the issues presented above, this TM provides information on the scientific background and computational details of a one-dimensional ecological ocean model for equatorial and mid-latitude applications. The model can read velocity components (u, v, w) and water temperature (T) from external sources, such as field observations or Ocean General Circulation Models (OGCMs), or calculate its own ocean temperature profile using one-dimensional mixed layer models (MLMs). There are two choices for the MLMs: the Chen MLM [Chen et al., 1994] and the Garwood MLM [Garwood, 1977]. In general, the Chen MLM is used in oceanic areas where vertical mixing is predominantly controlled by vertical shear, such as the Equatorial Pacific. Conversely, the Garwood MLM was successfully applied to mid-latitude areas, such as OWS P (50°N and 165°E), where vertical mixing is predominantly controlled by convective processes.

The following sections provide an overview of the modeling strategy, and a description of the model configuration and parameterization to make the user familiar with the model code, pre- and post-processing tools, and graphics interfaces that generalize the model applications.

1. Overview of Modeling Strategy

1.1 Atmospheric and Marine Optical Models

As will be described in the following sections, the ecosystem model requires solar irradiance forcing for the physical and biological components. Two methods are described here, the Frouin et al. [1989] model and the Gregg and Carder [1990] model. The descriptions of these two models, and their respective adaptations to the applications at hand, were reproduced from McClain et al. [1996] and McClain et al. [1998, submitted], respectively.

1.1.1 Non-Spectral, Clear Sky Scheme

Frouin et al. [1989] estimated the downwelling clear sky solar irradiance E_{clear} for two spectral domains, 350–700 nm (photosynthetically available radiation, PAR) and 250–4000 nm (total spectrum). PAR, rather than spectral irradiance, can be used to drive phytoplankton growth in low biomass (Morel and Prieur, [1977]) waters where only one phytoplankton species of constant specific absorption is assumed. In fact, simulations using a full spectral version of the coupled ecosystem model produced nearly identical monthly climatological chlorophyll a and temperature profiles to the OWS P application study, but at significant computational expense.

The near-infrared irradiance is calculated using the approximation

$$E_{clear}(700-4000) \cong E_{clear}(250-4000) - E_{clear}(350-700).$$ (1)

The error introduced by including the irradiance between 250 and 350 nm is small.

The model input includes ozone concentration, aerosol type (marine and continental), and visibility. A constant ozone concentration of 340 Dobson units is used, and the aerosol type is assumed to be marine. Visibility (V) is computed at each time step from the relative humidity (for the range of 65% to 99%) using the equation (Neuberger, [1951]):

$$V = 231 - 2.3RH,$$ (2)

where RH is the relative humidity (in percent). For $RH < 65\%$, $v = 80$ km, RH is determined using

$$RH = \frac{100e_{dp}(T)}{e_a(T)},$$

(3)

where e_a is the vapor pressure at the observed temperature and e_{dp} is the vapor pressure at the observed dew point temperature (Smith, [1966]). Vapor pressure is related to temperature by

$$e(T) = a_o e^{\frac{a_1 T}{(a_2 + T)}},$$

(4)

where $a_o = 6.1078$, $a_1 = 17.269$, $a_2 = 237.29°$, and T is the temperature (degrees Celsius) of either air or water [Tetens, 1930].

The irradiance that penetrates the ocean surface, $E(0^-)$, which is a function of the clear sky irradiance attenuated by cloud effects (see the calculation of E_{surf} in Section 1.1.3), is computed as

$$E(0^-) = (1 - \mu)E_{surf},$$

(5)

where μ is the surface reflectivity. The surface reflectivity consists of three components,

$$\mu = \mu_d + \mu_f + \mu_{ss},$$

(6)

where μ_d is the direct specular reflectance, μ_f is the reflectance from foam, and μ_{ss} is the subsurface reflectance due to molecular and particulate backscatter. The direct reflectance is taken to be the Fresnel reflectance for a flat surface unless the solar zenith angle is greater than $40°$ and the wind speed, W, is greater than 2 m s^{-1}. If these two conditions are satisfied [Austin, 1974], then

$$\mu_d = 0.0253e^{b(\theta_o - 40)},$$

(7)

where θ_o is the solar zenith angle and

$$b = -0.000714W + 0.0618.$$

(8)

The foam reflectance is computed as the product of the effective reflectance of foam (0.22 [Koepke, 1984]) and the wind-speed–dependent fraction of the surface covered by foam [Monahan and O'Muircheartaigh, 1980] or

$$\mu_f = 6.49x10^{-7}W^{3.52}.$$

(9)

For 0.01< chlorophyll a < 0.5 mg m^{-3}, μ_{ss} is approximately 0.035 [Morel, 1988].

After obtaining $E(0)$, the downwelling irradiance at depth z (the vertical coordinate decreases in the downward direction) is estimated by

$$E(z) = E(z - \Delta z)e^{-K(z)\Delta z},$$

(10)

where K is the downwelling diffuse attenuation coefficient. The K associated with each wavelength domain, PAR and the near-infrared, is determined independently. $K(PAR)$ is computed as a function of the chl a concentration at each depth (Morel [1988]; see also Wroblewski and Richman [1987] and Frost [1993]):

$$K(z, PAR) = K_w(PAR) + 0.0518chl(z)^{0.428},$$

(11)

where K_w (PAR) is the effective clear water diffuse attenuation coefficient (0.027 m^{-1}) and chl(z) is the chlorophyll a concentration at depth z. It should be noted that the monthly mean profiles of PAR obtained from this formulation were not substantially different from those obtained when integrating the spectral version of the model from 400 to 700 nm. For the near-infrared, K (NIR) is the effective value of K_w (NIR) over the wavelength band of 700–4000 nm and is assumed to be a constant ≈ 2.5 m^{-1} (Baker and Smith,

[1982]). The two wavelength bands are handled separately in the heat absorption calculation. The near-infrared radiation is essentially captured within the first meter of the water column.

The rate of heating at a given depth because of the absorption of downwelling irradiance is given by

$$\frac{dT(z)}{dt} = \frac{\{[E(z-\Delta z,\text{PAR}) - E(z,\text{PAR})] + [E(z-\Delta z,\text{NIR}) - E(z,\text{NIR})]\}\Delta z}{\rho_w c_{pw}} \quad (12)$$

where ρ_w and c_{pw} are the density and heat capacity, respectively, of water.

1.1.2 Clear Sky Spectral Atmospheric and Marine Optical Schemes

The model of Gregg and Carder [1990] can be used to compute the clear sky irradiance in the visible from 280–700 nm. The published version of the model only includes 350–700 nm (PAR), but is easily extended to include shorter wavelengths given the solar constants and ozone absorption coefficients for those wavelengths. Gregg and Carder's algorithm requires estimates of surface wind speed (from the European Center for Medium Range Weather Forecasting [ECMWF] monthly data), relative humidity (from Bishop and Rossow [1991]), precipitable water (from the International Satellite Cloud Cover Project [ISCCP]), visibility (from Bishop and Rossow [1991]) and ozone concentrations (from ISCCP).

1.1.3 Cloud Cover Corrections

Three different approaches for incorporating cloud cover effects on the radiative transfer models were used: two of these approaches were specifically designed for OWS P and the Warm Pool applications, whereas the third approach, developed by Tai and McClain [1996], is only possible when broadband, clear sky radiance observations are available for the region of interest and time period of simulation. The algorithm of Frouin et al. [1989] is used to calculate the total and PAR radiances for clear skies if observations are not available. A four-year (1987–1990) comparison was conducted between the total clear sky radiance provided by the Frouin et al. [1989] method and the equivalent clear sky radiance provided by Bishop and Rossow [1991]. The 4-year mean values of clear sky radiance derived from these two sources agree within 3% (295 W/m^2 from Frouin et al. [1989] and 303 W/m^2 from Bishop and Rossow[1991]).

The following is a description of the three different cloud cover corrections.

OWS P

This approach consists of an exponential fit to the fractional cloud cover. Cloud cover data for the period of January 1951 through December 1980 were obtained from the OWS P surface observation time series. These data have a resolution of 3 hours and vary from 6 oktas in autumn to 7.75 oktas in summer. By comparison, the COADS monthly mean cloud cover climatology has a similar pattern, with slightly higher values in autumn.

Clear sky irradiance is modified to account for the observed cloud cover by applying a power law correction tuned to yield the observed climatological monthly mean surface irradiances [Dobson and Smith, 1988],

$$E_{\text{surf}} = E_{\text{clear}}(1 - 0.53c^{0.5}), \quad (13)$$

where E_{surf} is the downwelling surface irradiance and c is the fractional cloud cover.

Warm Pool

Correcting the clear sky values for cloud cover is more difficult. For example, in the Warm Pool area, total surface irradiance observations from the TAO array are limited to August 1992 through April 1994. Total

monthly mean surface irradiance and cloud fraction estimates from the ISCCP [Schiffer and Rossow, 1985] are only available for July 1983 through June 1991. ISCCP surface PAR estimates [Bishop and Rossow, 1991] are not available for the time period of interest (1983–1992). Therefore, an algorithm for estimating the visible surface spectral irradiance from the theoretical clear sky irradiances and monthly mean ISCCP total irradiances and cloud cover was developed.

The approach emulated the ISCCP processing by using a proxy formulation which incorporates coefficients derived from statistical comparisons with ISCCP data. ISCCP total (tot) surface irradiance (250–4000 nm) and PAR are approximated using

$$E^{\cdot}(\text{tot}) = E_F^C(\text{tot})C_I^{\cdot}, \tag{14}$$

$$E^{\cdot}(\text{PAR}) = E_F^C(\text{PAR})C_I^{\cdot}, \tag{15}$$

where $E_I^{\cdot}$ (tot/PAR) is the equivalent ISCCP irradiance, E_F^c (tot/PAR) is the clear sky irradiance computed using the Frouin et al. [1989] algorithm, and $C_I^{\cdot}$ is the equivalent ISCCP cloud cover correction. The Frouin et al. [1989] algorithm requires water vapor (precipitable water), visibility, and ozone input. A marine haze model is assumed to be independent of wavelength, at least to the first order.

To estimate $C_I^{\cdot}$ using ISCCP cloud fraction data, the cloud correction scheme of Dobson and Smith [1988] is adopted, i.e.,

$$E_{DS}(\text{tot}) = E_o(\text{tot})[\cos\theta_o(A_i + B_i\cos\theta_o)], \tag{16}$$

where E_{DS} (tot) is the Dobson and Smith [1988] total irradiance, E_o is the extraterrestrial irradiance (1358.2 W m^{-2}), θ_o is the solar zenith angle, and A_i and B_i are empirical constants for each cloud okta (i.e., 0-8, okta = 0 will be designated as "c" for clear sky). Dividing (16) by (14) yields

$$\frac{E_{DS}(\text{tot})}{E_I(\text{tot})} = \frac{E_{DS}^c(\text{tot})C_{DS}}{E_F^c(\text{tot})C_I}, \tag{17}$$

where

$$E_{DS}^C(\text{tot}) = E_o(\text{tot})[\cos\theta_o(A_C + B_C\cos\theta_o)] \tag{18}$$

and

$$C_{DS} = \frac{A_i + B_i\cos\theta_o}{A_c + B_c\cos\theta_o}. \tag{19}$$

The values for the clear sky coefficients A_c and B_c are 0.40 and 0.386, respectively. The values for A_i and B_i vary according to the oktas.

Comparison of monthly mean values of E_{DS} computed using monthly mean cloud cover with E_I yielded a mean value of 1.11 for the left side of (17). Similarly, an annual cycle of E_F^c compared with E_{DS}^c values produced a fairly constant ratio of 0.95 for the first term on the right side of (17). It is assumed that these ratios are independent of wavelength and can be applied in the visible range.

Frouin et al. [1989] provided algorithms for both PAR and total surface irradiance while Gregg and Carder (1990) only addressed spectral PAR. Finally, the spectra for PAR can be expressed as

$$E_I(\lambda) = 0.85 R_{PAR} E^C_{GC}(\lambda) C_{DS} \tag{20}$$

where $R_{PAR} = E^c_F(PAR)/E^c_{GC}(PAR)$ at each time step. No smoothing of the monthly mean cloud fraction was included in the model surface irradiance computation. The 4-year mean (1987–1990) cloudy sky radiance derived from (14) is 243 W/m^2. This value is within less than 1% of the equivalent 4-year mean cloudy sky radiance (241 W/m^2) obtained from the Bishop and Rossow [1991] data set.

Cloud Attenuation Scheme using Observed Irradiances

When broad band *in situ* irradiance data are available, a more accurate scheme for cloud attenuation can be used. Leonard and McClain [1998, submitted] applied the scheme of Tai and McClain [1996], which is based on a combination of broad band irradiances derived from both irradiance models and field observations. The scheme uses a ratio between the broad band irradiance from the Tropical Atmosphere Ocean (TAO) buoy at 140°W on the equator (E_{OBS}), and the irradiance (E_F^C) calculated using the Frouin et al. [1989] broad band irradiance model. The modeled PAR was then multiplied by that ratio to obtain cloud-corrected PAR. Specifically,

$$E_{PAR} = E^C_{PAR} \left(\frac{E_{OBS}(tot)}{E^C_F(tot)}\right). \tag{21}$$

The modeled, cloud-corrected surface PAR compared well with *in situ* PAR data from the Joint Global Ocean Flux Study (JGOFS) equatorial Pacific cruises in 1992, validating the assumption that the attenuation of light by clouds is not strongly wavelength dependent.

1.2 The Garwood MLM

As mentioned in the Prologue of this TM, the Garwood [1977] mixed layer model was used to simulate mixed layer dynamics for the OWS P study because it performs best in oceanic areas where mixing is predominantly controlled by vertical convection, e.g., mid latitudes.

Garwood [1977] developed a one-dimensional bulk model of the mixed layer of the upper ocean. The model includes an entrainment scheme dependent on the relative distribution of turbulent energy between horizontal and vertical components as a mechanism for both entrainment and layer retreat. The model has two key dynamical properties for the generation and dissipation of turbulent energy:

- The fraction of wind-generated turbulent kinetic energy partitioned to potential energy increase by means of mixed layer deepening is dependent upon layer stability, $H^* = h/L$, as measured by the ratio of mixed layer depth h to Obukhov length L. This results in a modulation of the mean entrainment rate by the diurnal heating and cooling cycle.

- Viscous dissipation is enhanced for increased values of the inverted Rossby number, $R_o^{-1} = h f / u_*$, where f is the Coriolis parameter and u_* the friction velocity for the water. This enables a cyclical steady state to occur over an annual period by limiting maximum layer depth.

The main model assumption is that the turbulence of the overlying mixed layer provides the energy needed to de-stabilize and erode the underlying stable water mass. The turbulent kinetic energy budget is, therefore, the basis for the entrainment hypothesis:

$$\frac{1}{2}\frac{\partial\left(\overline{u'^2}+\overline{v'^2}+\overline{w'^2}\right)}{\partial t} = -\left[\overline{u'w'}\frac{\partial U}{\partial z}+\overline{v'w'}\frac{\partial V}{\partial z}\right]+\overline{b'w'}-\frac{\partial}{\partial z}\left[\overline{w'\left(\frac{u'^2+v'^2+w'^2}{2}+\frac{p}{\rho_o}\right)}\right]-\varepsilon \approx 0. \quad (22)$$

where ε is the viscous dissipation, p is pressure, and the ensemble mean and fluctuating components are denoted by the upper and lower cases, respectively. If the terms in (21) are known throughout the boundary layer, then the evolution of the potential energy and density profile may be evaluated using the budget for mechanical energy. The buoyancy equation is generated from the heat and salt equations together with an equation of state

$$\rho = \rho_o\left[1-\alpha\left(\theta-\theta_o\right)+\beta\left(S-S_o\right)\right], \quad (23)$$

and the definition for buoyancy

$$b = g\left(\rho_o-\rho\right)/\rho_o. \quad (24)$$

In (22) and (23) θ is the potential temperature, S salinity and ρ the density, while α and β are the expansion coefficients for heat and salt, respectively, and g is the gravity.

The bulk equations to be solved are the vertically integrated (within the mixed layer depth h) equations for buoyancy and momentum

$$h\frac{\partial\langle B\rangle}{\partial t}+\Delta B\frac{\partial h}{\partial t}\Lambda = \frac{\alpha g Q_o}{\rho_o C_p}-\overline{bw'}(0). \quad (25)$$

$$h\frac{\partial\langle U\rangle}{\partial t}+\Delta U\frac{\partial h}{\partial t}\Lambda = fh\langle V\rangle-\overline{uw'}(0), \text{ and} \quad (26)$$

$$h\frac{\partial\langle V\rangle}{\partial t}+\Delta V\frac{\partial h}{\partial t}\Lambda = -fh\langle U\rangle-\overline{vw'}(0), \quad (27)$$

where Q_o is the surface heat flux, C_p is the specific heat of sea water at constant pressure, and Λ is the Heaviside step function. B, U, and V refer to the time averaged values of buoyancy and velocity components. The coordinate system has x positive to the east, y positive to the north and z positive upward. Three assumptions were made in this integration:

(i) Vertical fluxes are negligible below the mixed layer, therefore,

$$\overline{bw'}(-h-\delta) = \overline{uw'}(-h-\delta) = \overline{vw'}(-h-\delta) = 0.$$

(ii) The mixed layer is sufficiently homogeneous so that

$$\Delta B \approx \langle B\rangle - B(-h-\delta)$$
$$\Delta U \approx \langle U\rangle - U(-h-\delta)$$
$$\Delta V \approx \langle V\rangle - V(-h-\delta)$$

(iii) Horizontal homogeneity is assumed for all mean variables.

1.3 The Chen et al. [1994] MLM

The Chen et al. [1994] MLM is based jointly on the Kraus–Turner type mixed layer model and Price et al. [1986] dynamical instability model. The scheme is computationally efficient and is capable of simulating the three major mechanisms of vertical turbulent mixing in the upper ocean, e.g., wind stirring, shear instability, and convective overturning.

The model ocean is divided into a fixed number of layers. The first layer represents the mixed layer, and the layers below the mixed layer are chosen according to a σ coordinate. In this fashion, the thickness of all layers is allowed to change, but the ratio of each σ layer to the total water column below the mixed layer is fixed to its prescribed value. Once the mixed layer depth is predicted, the thickness of the remaining layers are calculated diagnostically. The real advantage of such vertical coordinate system is its computational efficiency. Finer vertical resolution is assigned where it is needed, i.e., below the mixed layer [Gent and Cane, 1989]. This overcomes one of the disadvantages of the level models which need high resolution over the whole range of the mixed layer variation.

Since the layer interfaces are not material surfaces, there are fluxes of mass, buoyancy, and momentum through these interfaces. Of particular importance is the interface between the mixed layer and the layer right below, because the fluxes through it are directly related to the atmospheric forcing at the ocean surface.

The one-dimensional model equations are

$$\frac{\partial}{\partial t}(h_k \mathbf{u}_k) + (w\mathbf{u})_{k-1/2} - (w\mathbf{u})_{k+1/2} + f\mathbf{k} \times h_k \mathbf{u}_k = \tau_{k-1/2} - \tau_{k+1/2} ,$$ (28)

$$\frac{\partial}{\partial t}(h_k b_k) + (wb)_{k-1/2} - (wb)_{k+1/2} = B_{k-1/2} - B_{k+1/2} ,$$ (29)

$$\frac{\partial h_k}{\partial t} + w_{k-1/2} - w_{k+1/2} = 0$$ (30)

$$k = 1,2,......,nz$$

where $\mathbf{u}$ is the velocity vector, f is the Coriolis parameter, $\mathbf{k}$ is the unit vertical vector, τ is the wind stress, and B is the buoyancy flux. For simplicity, buoyancy b is assumed to be a linear function of temperature T. Thus (28) can be rewritten as

$$\frac{\partial}{\partial t}(h_k T_k) + (wT)_{k-1/2} - (wT)_{k+1/2} = Q_{k-1/2} - Q_{k+1/2}$$ (31)

where Q is the heat flux. A similar equation for salinity, S, can be included and b is determined from T and S using a simplified equation of state [Mellor, 1991]. Generally, τ and Q take the form

$$\tau_{k+1/2} = K_M^{k+1/2} \frac{(\mathbf{u}_k - \mathbf{u}_{k+1})}{h_k},$$

$$Q_{K+1/2} = K_T^{K+1/2} \frac{(T_k - T_{k+1})}{h_k} + I_{k+1/2},$$

$$(32)$$

where K_M and K_T are vertical eddy viscosity and diffusivity, respectively, and $I=rI_o e^{-Kz}$ is the penetrating solar radiation, where r is the fraction of the total irradiance, I_o, that is in the ultraviolet-visible portion of the spectrum, and K is the average diffuse attenuation coefficient for the ultraviolet-visible spectrum over the mixed layer. K and r are assumed to be constant by Chen et al. However, both are functions of time and K is a function of depth as well. The ecosystem model computes both r and K at each time step and the values can be provided to the mixed layer model in the coupled mode. At the top of the model, $\tau_{1/2}$ and $Q_{1/2}$ are specified as surface wind stress and heat flux; at the bottom of the model, $\tau_{nz+1/2}$ and $Q_{nz+1/2}$ are set to zero. The coefficients K_M and K_T are set to small constant values of background mixing ($K_M =1$ and $K_T = 0.1$ cm^2 s^{-1}). The principal turbulent mixing is caused by mixed layer entrainment, convection, and shear instability. The role of entrainment or detrainment is parameterized in (27) and (30) by the terms containing w. The convection and shear-produced mixing, however, are not explicitly included in (27) and (30); they are instantaneous convective adjustments.

1.3.1 Heat Budget Adjustment for the Chen et al. MLM

While simulating temperature profiles with the Chen et al. [1994] mixed layer model coupled with an ecosystem model (discussed below) in the Warm Pool, a slow warming trend was noticeable at all layers (0 to 250 meters). This warming trend was monotonic at about 6.3 x 10^{-8} °C s^{-1}, or 8°C in 4 years (the length of the simulation). Figure 1 shows the time series of $T(z)$; notice the downward trend of the isotherms towards the end of the simulation. Figure 2 shows the equivalent time series of $T(z)$ obtained from TOGA-TAO data at exactly the same location and time period. A comparison of Figures 1 and 2 reveals that the warming trend is obviously anomalous.

The authors attributed this anomalous warming trend to the limiting dynamics provided by the one-dimensional mixed layer model. The heat balance in the equatorial region cannot be accurately modeled without considering horizontal advection and diffusion terms. The one dimensional MLM does not exchange heat through the bottom of the vertical domain (250 meters). Therefore, the excess heat that would be exchanged laterally via the advection and diffusion terms in the three-dimensional thermodynamics, is constantly being accumulated in the one-dimensional vertical layers of the MLM.

To compensate for the anomalous warming, a strategy was developed to allow the excess heat to be flushed out from all layers of the MLM. This is an ad hoc but necessary strategy to ensure that an accurate $T(z)$ is provided to the ecosystem model. This strategy consists of an explicit finite difference for the heat equation that is applied at the end of each time step to $T(z)$ calculated implicitly by the original MLM thermodynamics. Specifically,

$$\frac{\partial T}{\partial t} = -w \frac{\partial T}{\partial z} + K_v \left(\frac{\partial^2 T}{\partial z^2} \right)$$

$$(33)$$

is subject to the following boundary conditions:

$$\left(\frac{\partial T}{\partial z} \right)_{z=0} = 0,$$

$$T(-h) = T_{bottom} = 14°C.$$

$$(34)$$

## Temperature in °C (No Flux Adjustment)
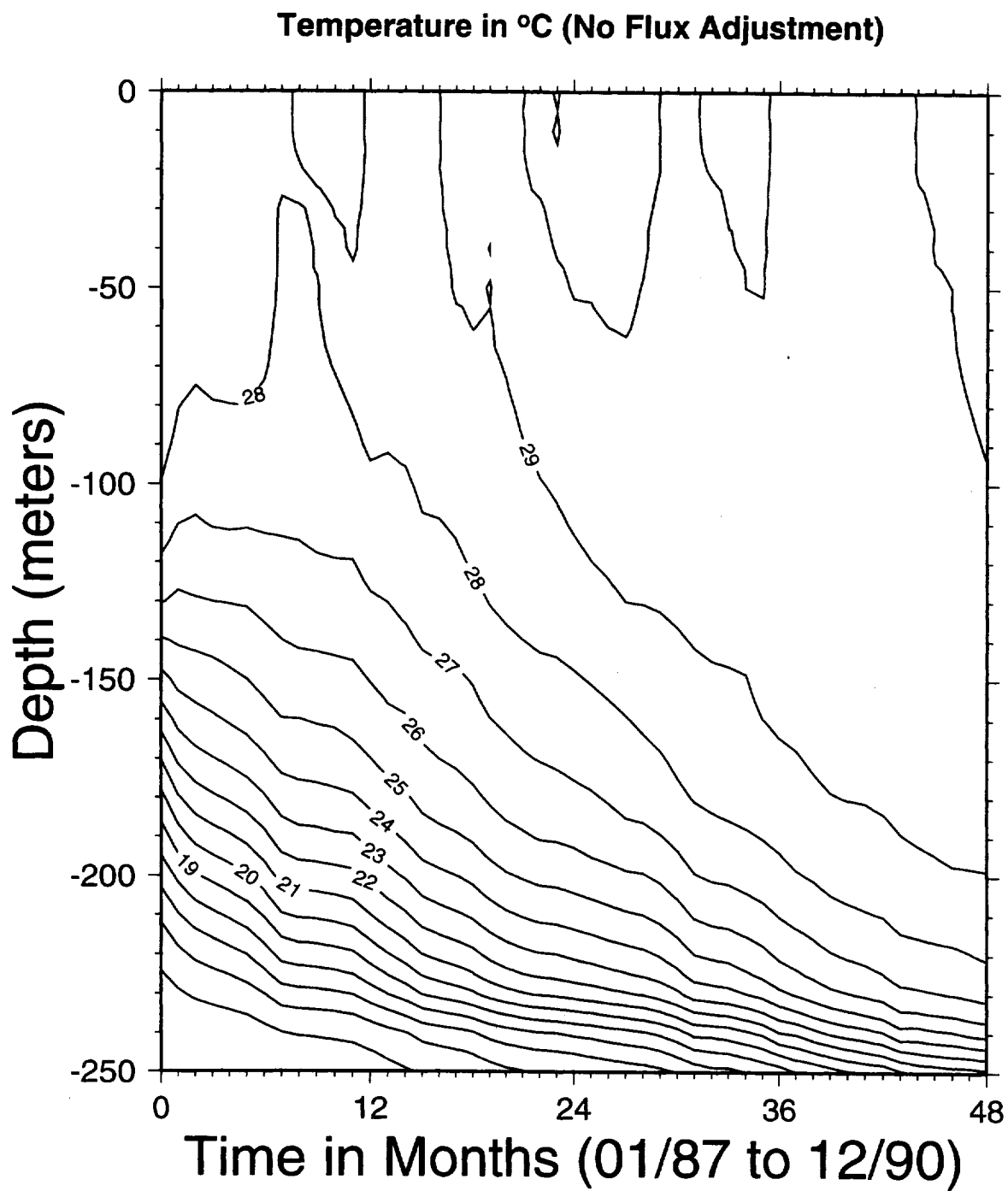
Figure 1. Four-year (1987–1990) time series of monthly-averaged MLM temperature at 165°E on the equator. The heat flux correction was not applied.

Temperature in °C (TOGA/TAO Data)
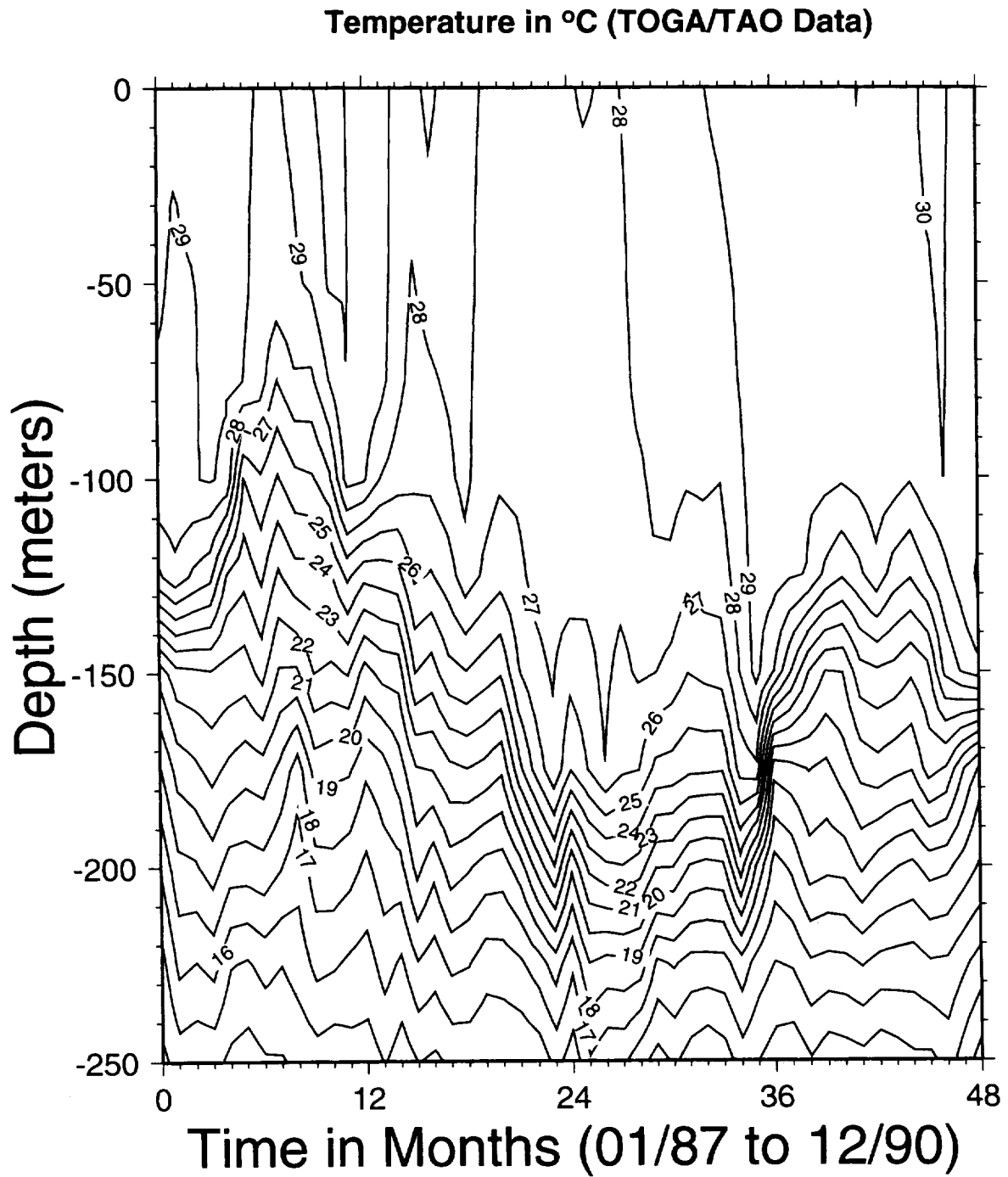
Figure 2. Four-year (1987–1990) time series of monthly-averaged TOGA–TAO temperature at 165°E on the equator.

The finite difference form of (32), which is up-wind in time and centered-difference in depth, can be written as

$$T^{n+1} = T^{n} - w^{n} \frac{T_{k}^{n} - T_{k+1}^{n}}{\Delta z} \Delta t + K_{v} \frac{T_{k-1}^{n} + T_{k+1}^{n} - 2T_{k}^{n}}{\Delta z^{2}} \Delta t \ , \tag{35}$$

where n is the time level, Δt is the time step, k is the index for the vertical level, and Δz is the layer thickness. Numerous sensitivity runs were conducted with different values of K_{v} to find the required value that compensates for the anomalous warming. The best value for K_{v} was 3.3 x 10^{-4} m^{2} s^{-1} (3.3 cm^{2} s^{-1}). Figure 3 shows a time series of $T(z)$ after the heat flux correction has been applied. Note that the isotherms are now in much closer agreement with the TOGA–TAO time series shown in Figure 2. Also, in Figure 4, a comparison is shown between the time series of T at 250 meters from the MLM and the time series of T at 250 meters from TOGA–TAO, before and after the heat flux correction (top tier and lower tier, respectively). Note that the warming trend has been completely removed from the record once the heat flux adjustment has been applied.

To verify how realistic this heat flux would be in terms of an equivalent horizontal flux, the required zonal temperature gradient for heat advection, $u \partial T / \partial x$, is calculated and the result with values of zonal temperature gradients derived from TOGA–TAO data are compared. At 250 meters, the zonal component of the velocity, u, averages 20 cm s^{-1} (from TOGA–TAO data). With this value of u, the required $\partial T / \partial x$ that matches the adjustment value of 6.3 x 10^{-8} °C s^{-1} is 3.2 x 10^{-7} °C m^{-1}, or 0.032 °C/100 km. According to Wang and McPhaden [1998], zonal temperature gradients of this magnitude are easily found in the Warm Pool area and, therefore, the hypothesis of heat leakage via horizontal advection is a feasible thermodynamic mechanism in the heat budget of the western equatorial area.

1.4 The Ocean General Circulation Model (OGCM)

The OGCM is the reduced gravity, primitive equation, σ coordinate model of Gent and Cane [1989] with an embedded hybrid mixing scheme of Chen et al. [1994]. Surface heat fluxes are computed by coupling the OGCM to an advective atmospheric mixed layer model (Murtugudde et al., [1996]). Complete hydrology has been added to the model with freshwater forcing treated as a natural boundary condition (Huang, [1993]). The UNESCO equation of state is used for computing buoyancy from salinity and temperature. The improvements in tropical SST simulations and upper ocean hydrology was reported in Murtugudde et al. [1995] and Murtugudde and Busalacchi [1997], respectively. The vertical structure of the model ocean consists of a mixed layer and a specified number of layers below according to a σ coordinate (total number of layers is 20 for the Warm Pool simulation). The horizontal grid is stretched down to 1/3° resolution near the equator and at the eastern and western boundaries. The model domain spans the Pacific zonally with meridional boundaries at ±30° latitude. The mixed layer depth and the thickness of the last σ layer are computed prognostically and the remaining layers are computed diagnostically such that the ratio of each σ layer to the total depth below the mixed layer is held to its prescribed value. The model has a 1-hour time step and 10-day average velocity, temperature, and mixed layer values are output for use in ecosystem models with one-way coupling. The model is spun up with climatological winds for 10 years. The interannual simulation for 1983–1992 is initialized with the climatological run and forced with the monthly mean Florida State University (FSU) winds. The precipitation data of Xie and Arkin [1996] was used for freshwater forcing.

1.5 One-Way Coupling with Ocean Global Circulation Model

The ecological model can be driven by velocity (u,v,w) and water temperature fields (T) originating from the OGCM output. In this manner, the OGCM is configured and runs independently from the ecological

Temperature in °C (Kv = 0.000333 m²/s)
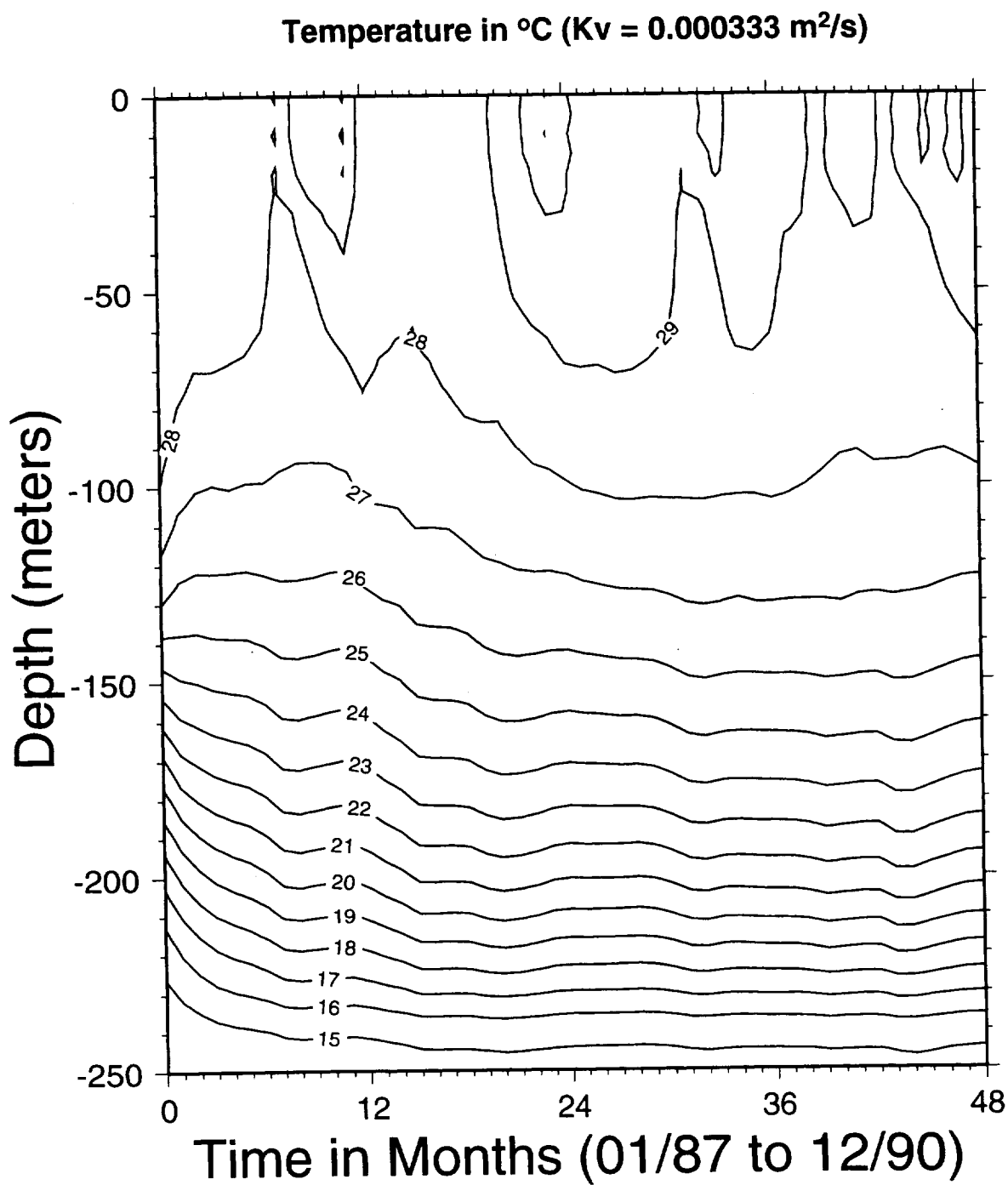
Figure 3. Four-year (1987–1990) time series of monthly-averaged MLM temperature at 165°E on the equator. The heat flux correction was applied.
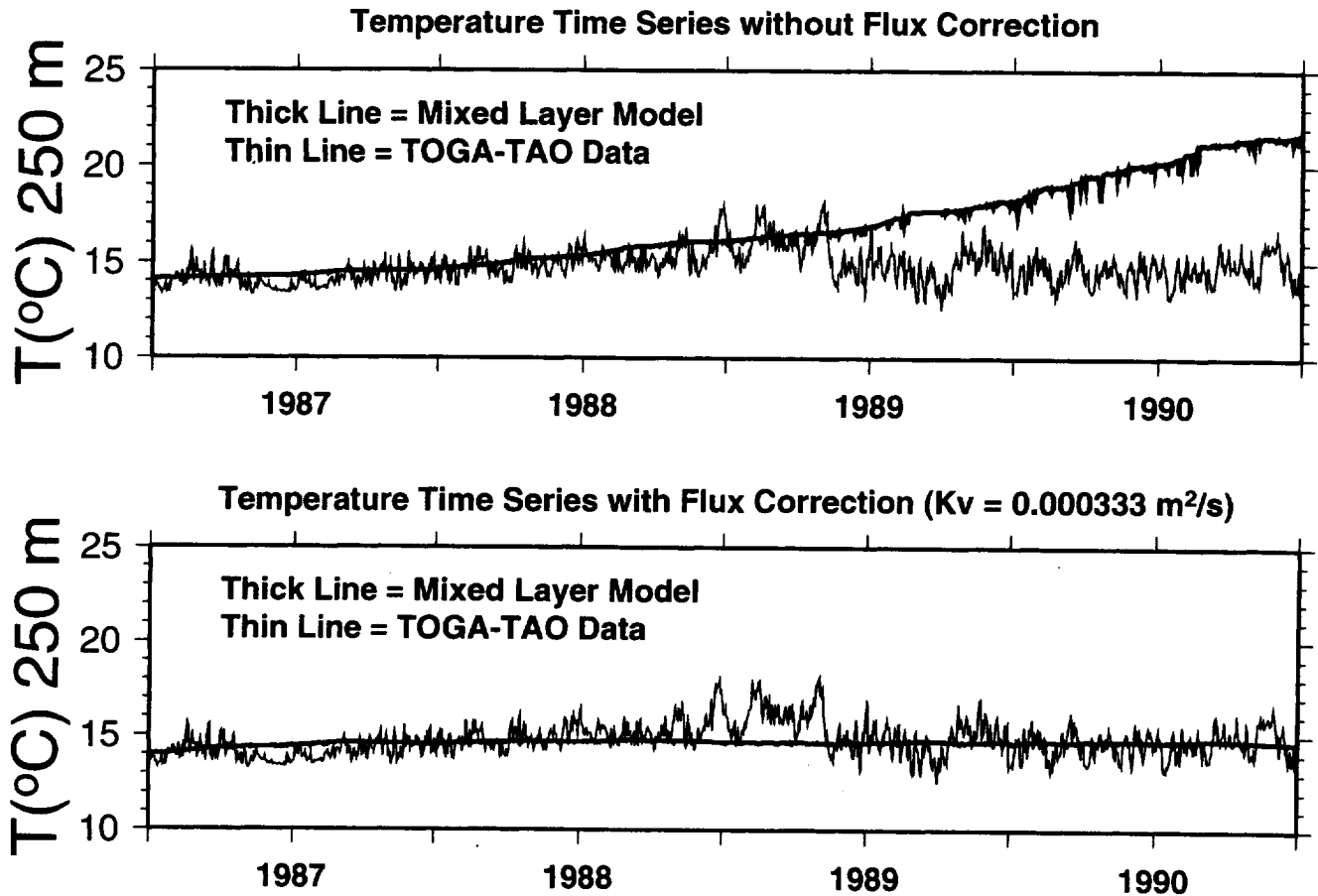
Figure 4. Four-year (1987–1990) daily time series of TOGA–TAO and MLM temperature at 250 m. The upper tear shows the comparison between the MLM temperature without heat flux correction and the TOGA–TAO temperature. The lower tear compares the MLM temperature using the heat flux correction and the same TOGA–TAO temperature time series. Note the elimination of the warming trend in this lower tear.

model; the u, v, w, and T fields are stored at preset time intervals (in this case, 10 day averages) for subsequent use as input to the ecological model   The ecosystem model is executed at one hour intervals with OCGM input derived from a linear interpolation of the 10-day average values. Other combinations for the driving physical fields have also been tried. An example is the usage of the vertical velocity component from the OGCM and u, v, and T fields from the TOGA moorings. Figure 5 shows the processing flow when the ecosystem model is linked to either a mixed layer model (coupled mode) or is forced by prescribed input (uncoupled or 1-way forcing mode).

1.6 Ecosystem Model

The ecosystem model (Figure 5) is essentially the same as that used in McClain et al. [1996] with the following modifications:

1. The light model used in the Warm Pool and OWS P applications includes spectral absorption from 280 to 700 nm. The spectral light model requires absorption spectra for water and chlorophyll a. The seawater absorption spectrum of Baker and Smith [1982] was used.   The use of a spectral model eliminated the need to estimate light attenuation for PAR, i.e., K(PAR), using the Morel [1988] empirical function based on chlorophyll-a concentration. Also, the growth rate and C:Chl (carbon to chlorophyll a) ratio computations require integration over PAR in units of μmol quanta. The transformation from W m^{-2} nm^{-1} to μmol quanta m^{-2} s^{-1} nm^{-1} was applied to each wavelength according to the expression (Zeebe et al., [1996])

$$E^{\mu mol}(\lambda) = \frac{E^W \lambda 10^6}{N_a hc},$$ (36)

where N_A is the Avogadro number ($6.022.10^{23}$), h is Planck's constant ($6.626.10^{-34}$ J s), c is the   speed   of light ($2.998.10^8$ m s^{-1}), and λ is in meters.

2. In the Warm Pool application, the surface-wind-stress-dependent algorithm for the eddy diffusion, K_v, has been replaced with the method of Pacanowski and Philander [1981], which uses profiles of temperature and horizontal currents (u and v) obtained from the OGCM.

3. In the Warm Pool application the vertical velocity, w, is obtained from the OGCM rather than being derived from the curl of the local wind stress.

4. In the Warm Pool application the bottom boundary (250 m) nitrate concentration is allowed to change as a function of temperature, T (° C). A variable bottom boundary condition was needed because, at the equator, planetary waves introduce significant vertical excursions of the isopycnal surfaces below 250 m. Using climatological nutrient data at 165°E from Conkright et al. [1994] for standard depths between 150 and 350 m,

$$NO_3 = 39.64 - 1.467T$$ (37)

with an $r^2 = 0.92$.

5. For simulations in the Warm Pool, the exponential temperature-dependent zooplankton respiration rate (r_z) algorithm was replaced with a linear relationship based on data from Ikeda [1985]. The linear respiration relationship,

$$r_z = 0.0722 + 0.0067(T - 20),$$ (38)
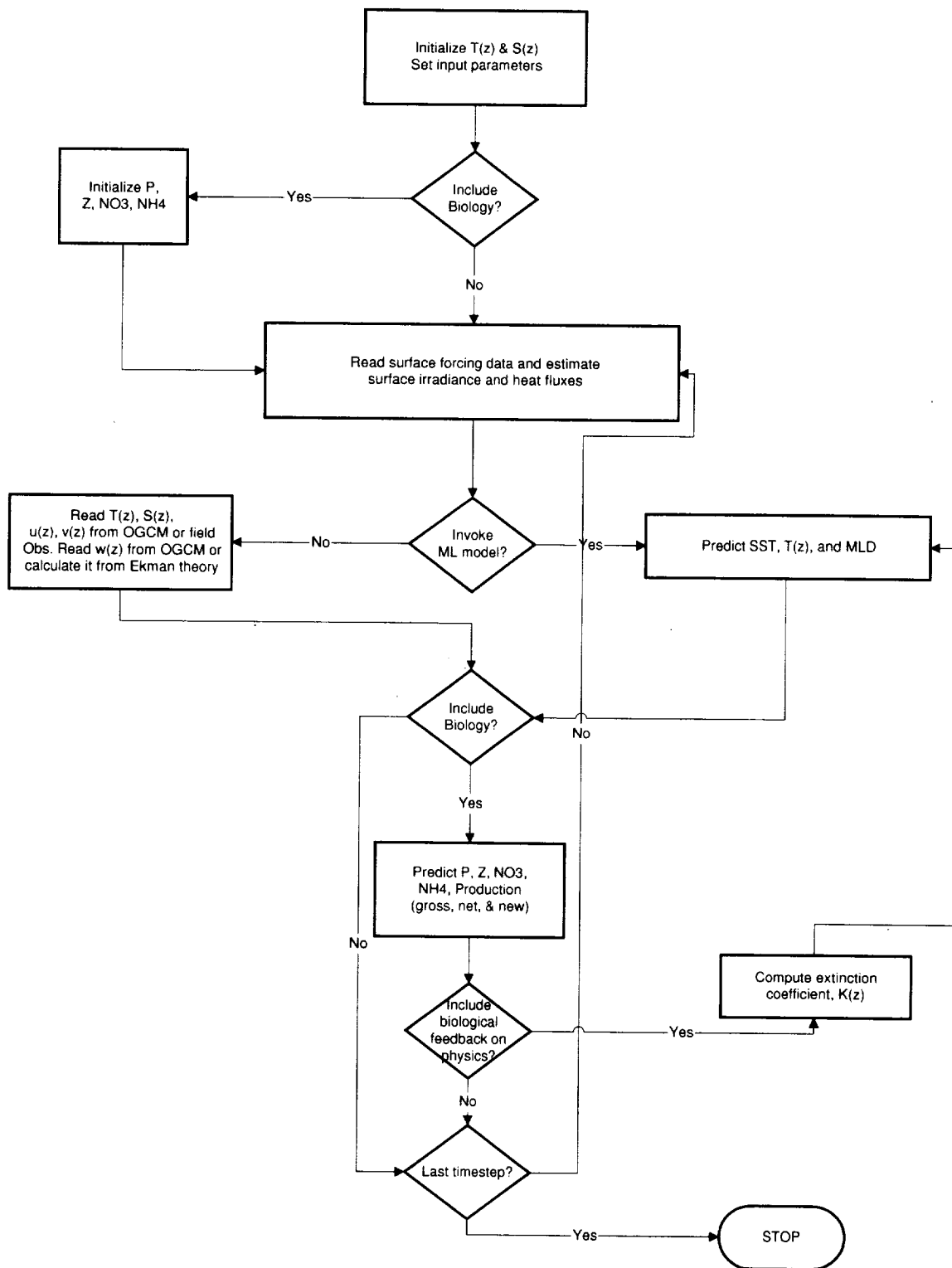
Figure 5. Flow chart of ecosystem model showing the processing flow and the linkage between the four component biological model with the physical fields. The chart shows two options for the use of the physical fields: one originating from the one-dimensional MLM and another originating from the OGCM.

produces rates of less than 0.15/day.

6. In the Warm Pool application, the half saturation constant for NH_4, K_{NO_3}, was increased from 0.1 to 0.5. Also, the NH_4 inhibition coefficient, pk, was increased from 3 to 5. These changes were introduced to help limit growth rates to a range consistent with observed values since maximum growth rates predicted by the Eppley [1972] expression are ≈ 5 d^{-1} for the surface temperatures in the Warm Pool.

7. For the Warm Pool simulations, phytoplankton mortality, m, was increased from 0 to $0.1 d^{-1}$ to obtain phytoplankton concentrations more consistent with observations. Also, zooplankton mortality was increased from 0.04 to 0.15 d^{-1} to obtain a pronounced subsurface chlorophyll maximum.

8. The phytoplankton sinking rate was set to zero to reflect the fact that cell sizes are relatively small in the Warm Pool [Blanchot et al., 1992].

9. The C:Chl a ratio in the Warm Pool application was limited to the range 20–300 to be consistent with the observed range of values [Furuya, 1990; Chavez et al., 1991] for the equatorial Pacific.

10. In both Warm Pool and OWS P applications, fecal pellet remineralization (conversion to NH_4) was added as a constant fraction (c_{pel}) of the fecal pellet production. About 70% of the pellets are recycled in the photic layer of the HNLC (high nutrient–low chlorophyll; Dam et al., 1995) and 84% [Le Borgne and Rodier, 1996] in the oligotrophic regimes of the equatorial Pacific. A value of $c_{pel} = 0.8$ was used.

11. For both Warm Pool and OWS P simulations, an ammonium nitrification algorithm based on Olson [1981] was incorporated. The strategy is to model irradiation dosage between 300–470 nm to inhibit bacterial conversion of NH_4 to NO_3 near the surface. The addition of this process was prompted by the buildup of NH_4 at depths below the observed subsurface NH_4 maxima between 60–120 m (James Murray, personal communication). The rate of conversion of ammonium to nitrate, A^n (nmol/day) is

$$A^n(z) = A^n_{max}(z)\left[\frac{D(z) - D_{min}(z)}{D(z) - D_{min}(z) - K_D(z)} - 1\right], \tag{39}$$

where

$$D(z) = \frac{1}{T}\int_0^T \int_{300}^{470} E_S(z, \lambda, t).as(\lambda).d\lambda dt \tag{40}$$

T is 24 hours, $D_{min} = 0.0095$ W/m^2, $A^n_{max} = 2$ nmol/day, $K_D = 0.036$ W/m^2, and E_s has units of W/m^2/nm. K_D is the half saturation dosage or the dosage at which inhibition is half the maximum rate, and D_{min} is the minimum inhibition dosage. The absorption coefficient for NH_4, $as(\lambda)$, was digitized from Figure 3 of Olson [1981] which provides the action spectra for photoinhibition of *Nitrobacter winogradskyi* and *Nitrosomonas europaea*; the photoinhibition spectrum for the latter species was used.

The following system of coupled differential equations simulates the dynamics of phytoplankton nitrogen (P), micro-zooplankton nitrogen (Z), ammonium (NH_4), and nitrate (NO_3) stocks within the upper ocean:

$$\frac{\partial P}{\partial t} + w_c\frac{\partial P}{\partial z} + \frac{\partial SP}{\partial z} - \frac{\partial}{\partial z}\left(K_v\frac{\partial P}{\partial z}\right) = GP - mP - r_pP - IZ , \tag{41}$$

$$\frac{\partial Z}{\partial t} + w_e \frac{\partial Z}{\partial z} - \frac{\partial}{\partial z}\left(K_v \frac{\partial Z}{\partial z}\right) = (1 - \lambda)IZ - gZ - r_z Z, \tag{42}$$

$$\frac{\partial NH_4}{\partial t} + w_e \frac{\partial NH_4}{\partial z} - \frac{\partial}{\partial z}\left(K_v \frac{\partial NH_4}{\partial z}\right) =$$

$$\left(a_{pm} + r_p - \pi_1 G\right)P + \left(a_z g + r_z + c_{pel}\lambda I\right)Z - A^n, \tag{43}$$

and

$$\frac{\partial NO_3}{\partial t} + w_e \frac{\partial NO_3}{\partial z} - \frac{\partial}{\partial z}\left(K_v \frac{\partial NO_3}{\partial z}\right) = -\pi_2 GP + A^n. \tag{44}$$

Table 1 provides the variable definitions and the values of the free parameters used in deriving various terms in these equations. The rate of phytoplankton growth (G), the herbivore grazing term (I), and the partitioning of NH_4 and NO_3 uptake (π) are calculated using the following equations:

$$G = \beta G_m, \tag{45}$$

$$G_m = G_o e^{k_{gr}T}, \tag{46}$$

$$I = R_m[1 - e^{-\Lambda P}], \tag{47}$$

$$\pi_1 = \frac{NH_{4lim}}{NH_{4lim} + NO_{3lim}}, \tag{48}$$

$$\pi_2 = \frac{NO_{3lim}}{NH_{4lim} + NO_{3lim}}, \tag{49}$$

where, in (44) and (45), $G_m(d^{-1})$ is the first-order exponential function of temperature (Eppley, [1972]), G_o (d^{-1}) is the specific growth rate at $0°C$, k_{gr} ($°C^{-1}$) is a rate constant which determines the sensitivity of G_m to changes in T. β is the resource limitation term calculated as the smaller of the computed nutrient and light limitation terms (N_{lim} and L_{lim}, respectively). In (46), R_m is the maximum ingestion rate of zooplankton and Λ determines the sensitivity of grazing to phytoplankton stock. Ammonium (NH_{4lim}) and nitrate (NO_{3lim}) limitation are calculated using the standard hyperbolic formulation (Monod [1942]). More specifically, in Equations (47) and (48), the ammonium limitation term is calculated using the equation

$$NH_{4lim} = \frac{NH_4}{K_{NH_4} + NH_4}, \tag{50}$$

where K_{NH_4} is the NH_4 concentration where growth is half maximal. The nitrate limitation term is calculated in a similar manner but with the addition of a term to correct for inhibition of NO_3 uptake due to the presence of NH_4 (Wroblewski [1977])

$$NO_{3lim} = \frac{NO_3}{K_{NO_3} + NO_3} e^{-pkNH_4} , \qquad (51)$$

where K_{NO_3} is the NO_3 concentration where growth is half-maximal and pk determines the sensitivity of NO_3 uptake to the presence of NH_4. The nutrient limitation term, N_{lim}, is defined as the maximum value between NH_{4lim} and NO_{3lim}. The light limitation term, L_{lim}, is a function of the ambient irradiance and the photoadaptation parameter (McClain et al. [1996]).

The coordinate system origin is at the surface and negative downward. To prevent numerical instability when solving the finite difference form of the continuum equations above, the Crank–Nicholson scheme (Press et al., [1988]) was applied. This involves the simultaneous solution of these linear equations for each time step and each depth using the method of Gaussian elimination for tridiagonal systems. The Neumann boundary condition, $\partial X/\partial z = 0$, is applied at both the surface and lower (350 m for OWS P and 250 m for the Warm Pool) model domain boundaries for P and Z. Initial profiles of temperature and NO_3 are usually obtained from annual climatologies. Depth-independent initial concentrations of P, Z, and NH_4 are given in Table 1. For the OWS P study, NH_4 and NO_3 were given a fixed value equal to the initial condition at the lower boundary and the Neumann condition was applied at the surface.

2. Model Applications

2.1 Ocean Weather Station P, 1951-1980

Physical and biological processes in the mixed layer at OWS P ($50°N$, $145°W$) over a 30-year period (1951–1980) were investigated using observations and model simulations (McClain et al., [1996]). The observations include 30 years of surface meteorological and sea surface temperature data collected at OWS P and Ekman upwelling velocities derived from COADS, 14 years (1953–1966) of daily temperature profiles, nearly 150 chlorophyll a profiles spanning all months of the year, monthly climatological solar radiances, and 0- to 50-m integrated nitrate concentrations. The simulations incorporated models for the estimation of surface solar downwelling irradiance, surface heat fluxes, subsurface diffuse attenuation, mixed layer dynamics, and biological processes. The time-dependent model input was the surface observations of cloud cover, air temperature, dew point temperature, and wind speed. The atmospheric irradiance, marine diffuse attenuation, and mixed layer models were adapted from existing models developed by others.

The mixed layer depth (MLD) is calculated using an updated version of the Garwood [1977] one-dimensional dynamical MLM, as described in Section 1.1. This model predicts the rate of deepening or retreat of the mixed layer as a result of entrainment or detrainment processes at its lower boundary.

The biological model, developed by McClain et al. [1996], has four components (nitrate, ammonium, phytoplankton nitrogen, and zooplankton nitrogen) and computes a variety of additional quantities including chlorophyll a concentration and gross and new production. The non-spectral model produced seasonal climatological chlorophyll a profiles within the observed standard deviations at almost all depths, but with values markedly less than the mean observed values in some seasons, e.g., summer. Also, the non-spectral model did not include nitrification of NH_4 to NO_3 resulting in the accumulation of NH_4 at depth. Climatological monthly profiles of temperature were within one standard deviation of the observed values at nearly all depths. Also, the climatological annual cycles of solar irradiance and 0- to 50-m integrated nitrate accurately reproduced observed values. Annual primary production was estimated at ~190 g C m^{-2} yr^{-1} and varied by no more than $\pm5\%$ in any year. This estimate is consistent with recent observations but is much greater than earlier estimates, indicating that carbon cycling in the North Pacific is much more important to the global carbon budget than previously thought. Significant interannual variability in sea surface temperature, Ekman upwelling, mixed layer depth, and surface nitrate concentration had little

impact on productivity. The model results also indicated that the nitrate supply to the euphotic zone is very sensitive to Ekman upwelling and that amplification of the wind stress curl results in complete nitrate depletion when the winds are persistently downwelling favorable.

The 30-year simulation at OWS P was repeated using the spectral model (Figure 6) with the zooplankton mortality rate, g, adjusted to 0.07/day. This simulation produced improved seasonal chlorophyll a profile climatologies (Figure 7) where the elevated values in the boreal summer and fall are more accurately reproduced. While there are no profile data available for NH_4, the seasonal profiles shown in Figure 8 display subsurface maxima with zero values at depths which are independent of the bottom boundary condition. In the simulation of McClain et al. [1996], the subsurface maxima were solely a result of the small value assigned as the bottom boundary condition. Finally, Figure 9 illustrates the climatological annual time series of 0–60 meter average chlorophyll a (or P), Z, NO_3, and NH_4. The data displayed for NO_3 were taken from Frost [1991] and indicate that the simulated values are slightly high during the winter, but are in excellent agreement for the other seasons.

2.2 Equatorial Pacific Warm Pool at 165° W

A four-year simulation (1987–1990) of biological processes in the equatorial Pacific Warm Pool was performed using the 4-component (phytoplankton, zooplankton, nitrate, and ammonium) spectral ecosystem model described above with the input parameter values provided in Table 1.

The physical parameters (u, v, w, T) required by the ecosystem model, which are shown in Figures 10–13 were derived from the OGCM of Murtugudde and Busalacchi [1997]. Surface downwelling spectral irradiance was estimated using the algorithm described in Section 1.1.3 with ISCCP monthly mean cloud fraction data. The vertical diffusivity (Figure 14) was computed from the u, v, and T profiles using the method of Pacanowski and Philander [1981]. During 1987–1990, three deep mixing events occurred, all in the spring or early summers of 1988–1990. The observed u, v, and T time series are shown in Figures 15, 16 and 2, respectively. Zonal velocities from the OCGM are in general agreement with observations in terms of the magnitudes of the values and the phasing of the flow reversals in the upper 150 m. Meridional flow is relatively weak and the model does not emulate the observed values very well. The vertical velocity field exhibits a shallow upwelling maxima at about 50 m with alternating periods of upwelling and downwelling at depth. Particularly strong upwelling below 100 m occurred in late 1987 and 1990. The OCGM temperature field resembles the observed structure but is cooler by 1–3°C with larger differences occurring at depth.

Figure 17 summarizes the ecosystem response to physical forcing. The results clearly indicate that upwelling at 100 m is closely associated with surface blooms. For instance, the 100 m upwelling events in late 1987 and 1990 produced dramatic increases in the surface layer values of all four ecosystem components, whereas the spring-summer deep mixing events (K_v time series) do not seem to incur a response in any of the ecosystem quantities.
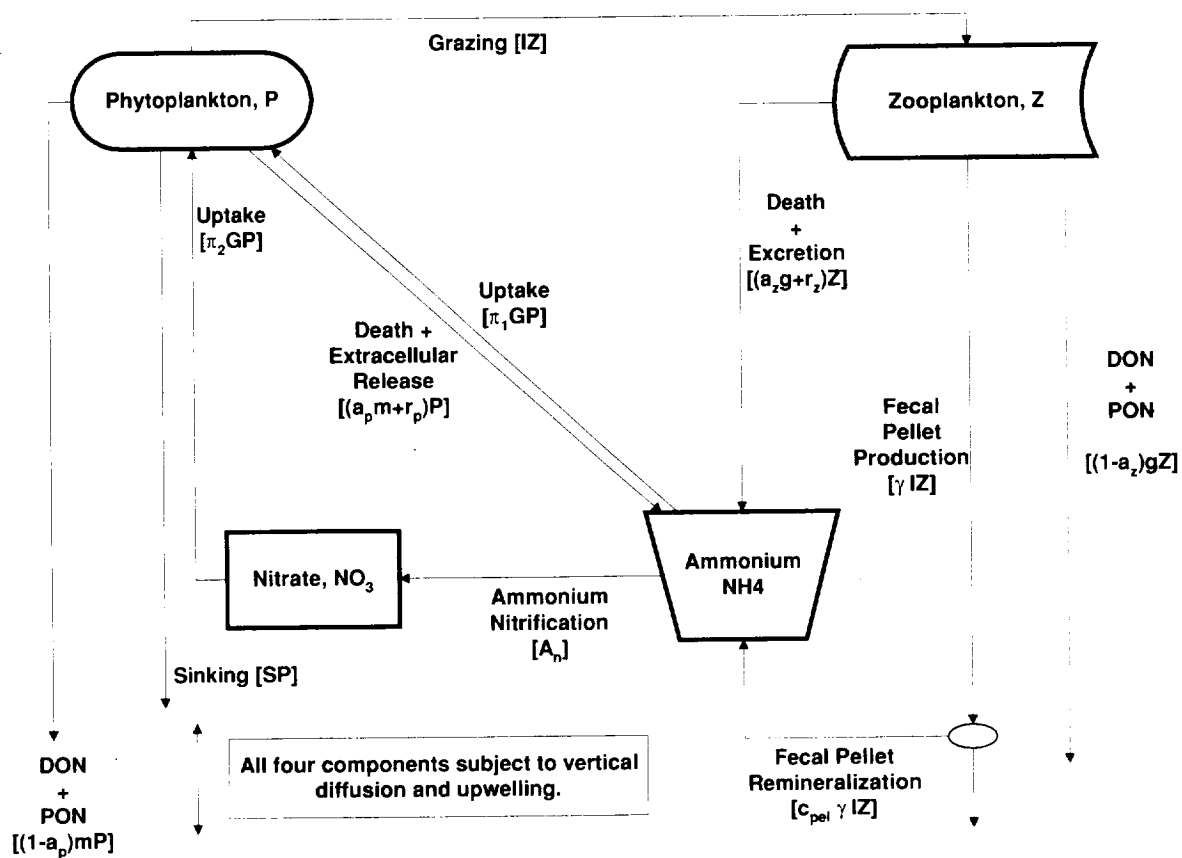
Figure 6. Diagram of four-component ecosystem model showing the bio-chemical interactions between components.

Phyto(mg Chl-a m⁻³)
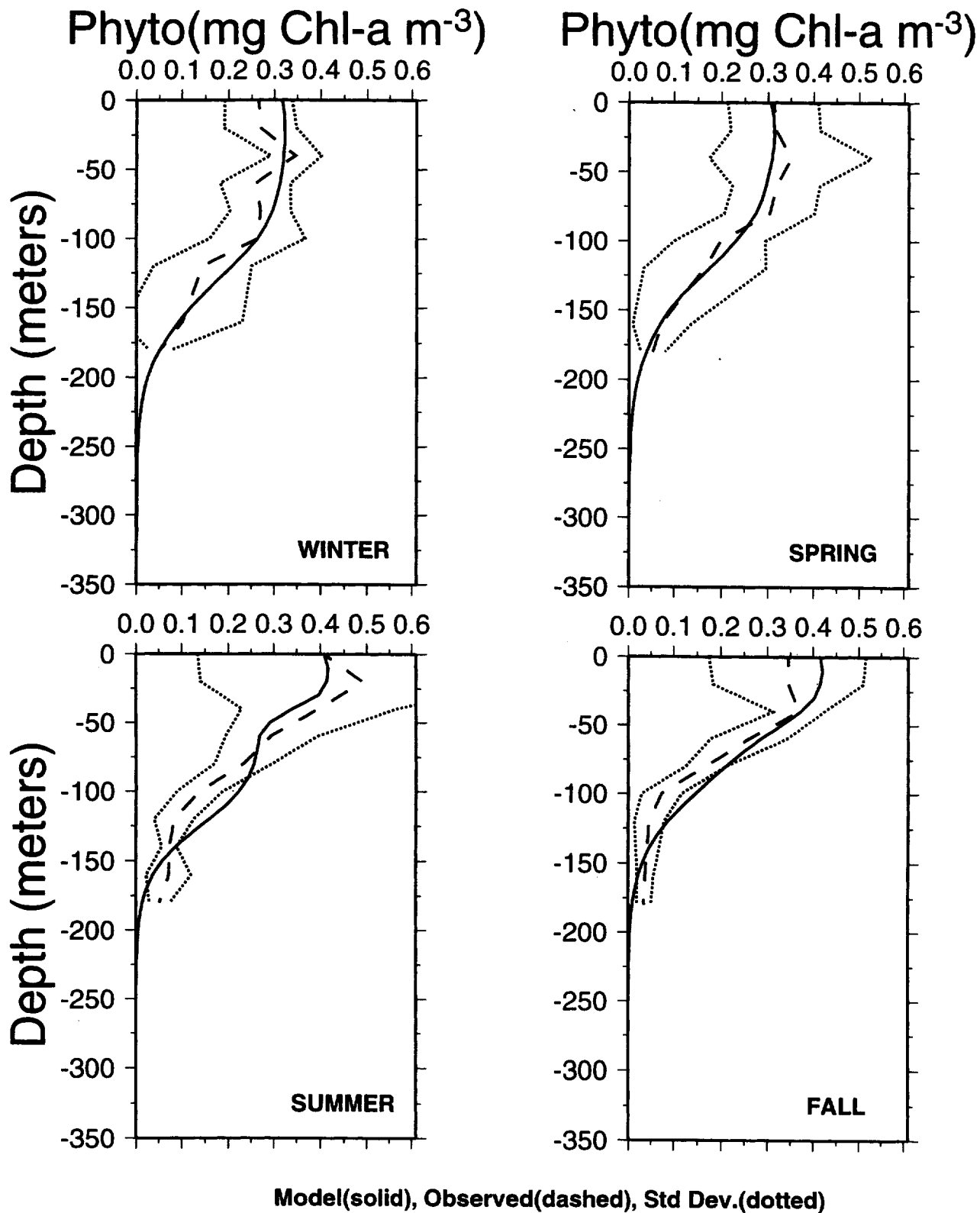
Figure 7. Seasonally averaged vertical profiles of phytoplankton concentration predicted by the ecosystem model at 50°N and 145°W (OWS P). The model profiles are the solid lines, the observed values are represented by the dashed lines, and the the standard deviation boundaries are shown by the dotted lines.
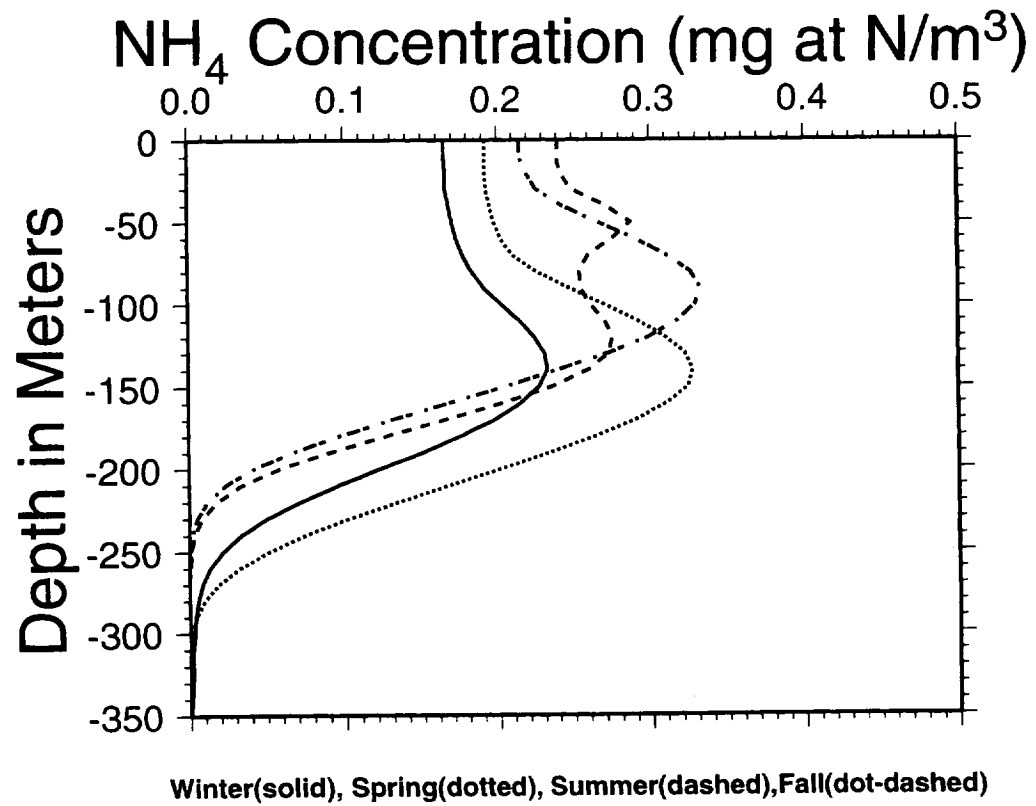
Figure 8. Seasonally averaged vertical profiles of ammonium concentration predicted by the ecosystem model at 50°N and 145°W (OWS P).
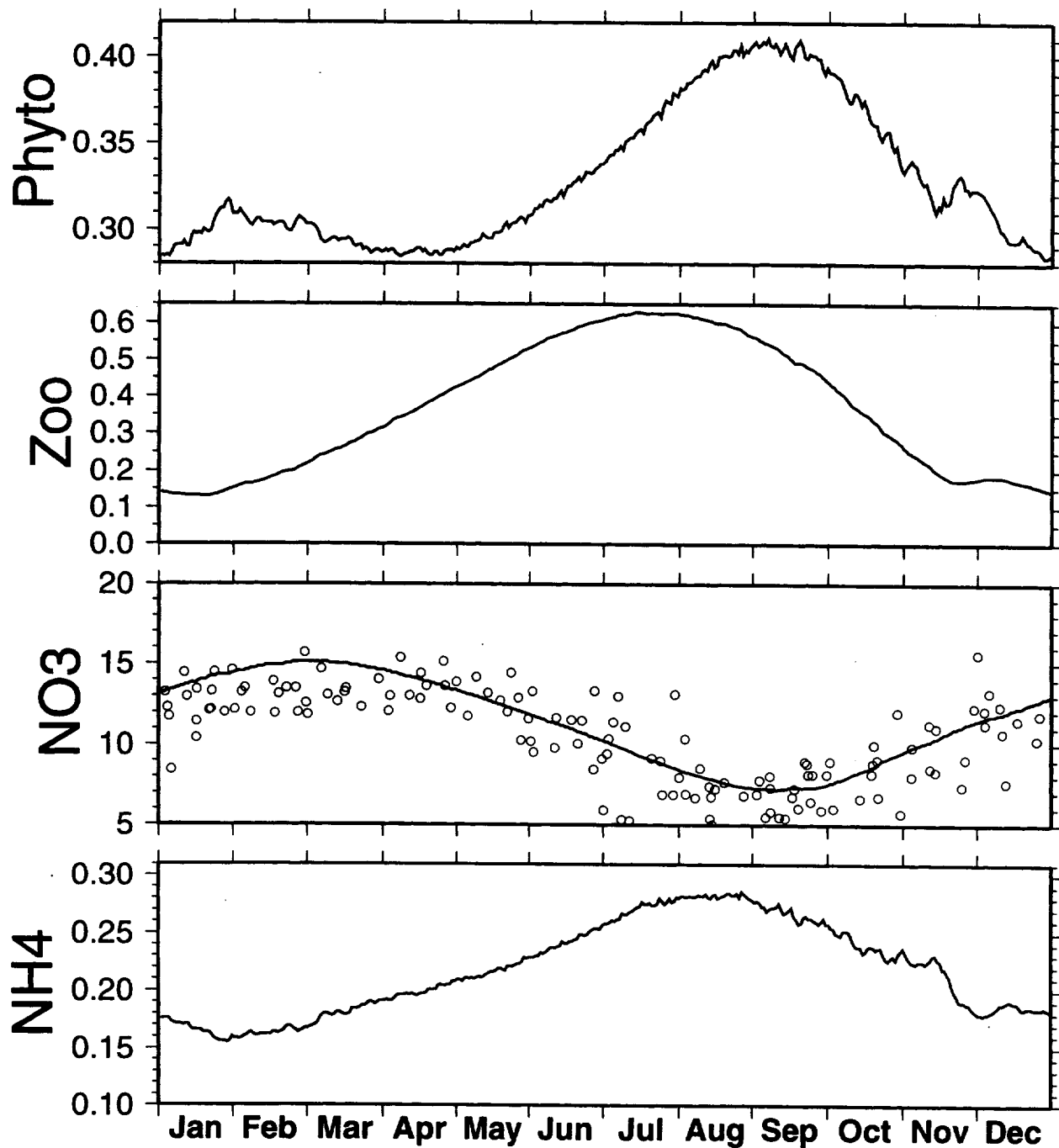
Figure 9. Composite time series plot of 30-year (1951–1980) vertically averaged (0–60 m) climatological concentrations of phytoplankton, zooplankton, nitrate, and ammonium. Note the large seasonal cycle of all bio-chemical components. The climatological seasonal cycle of nitrate concentration compares well with observed data (blank circles).

Zonal Velocity in cm/s (OGCM Simulation)
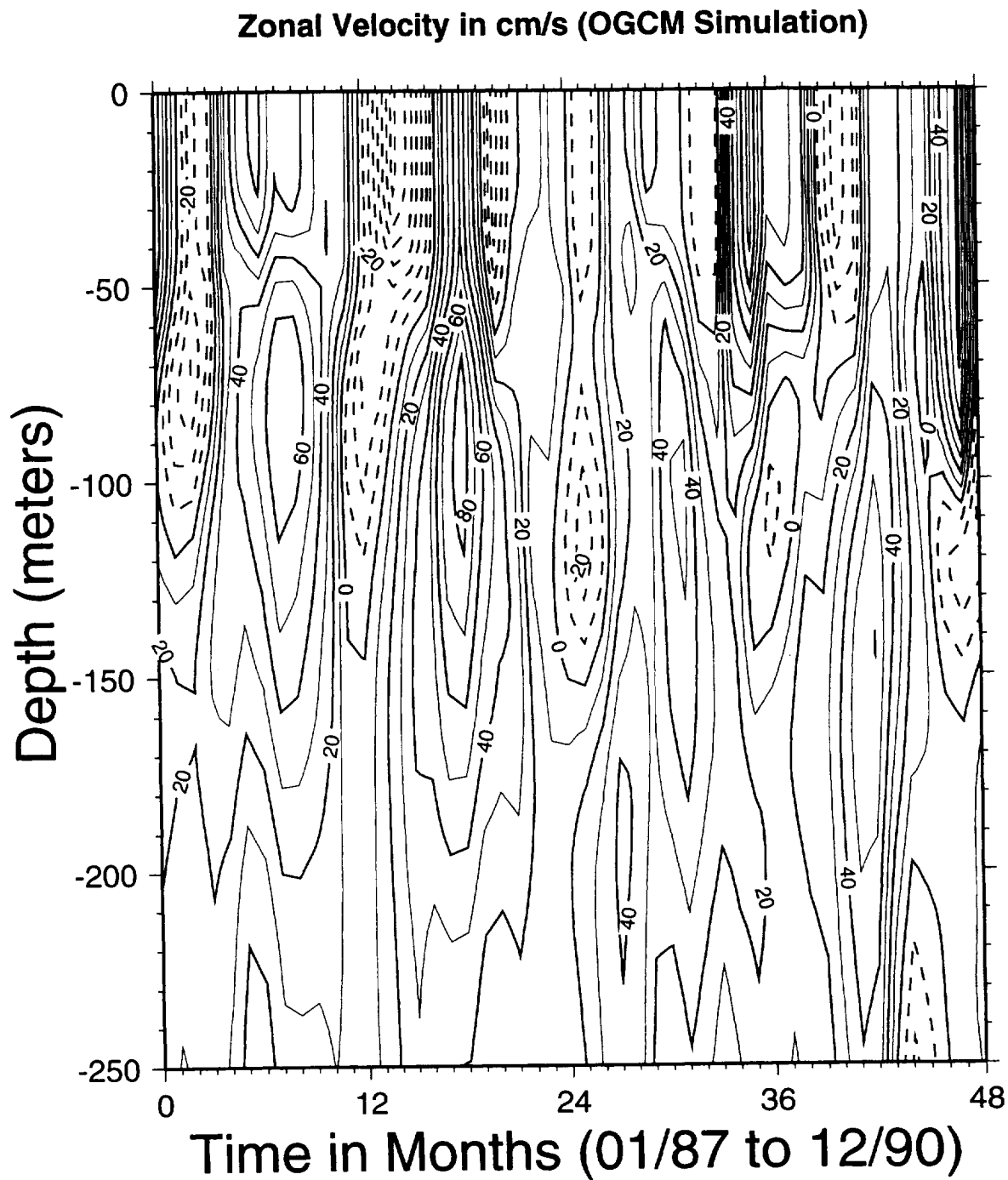
Figure 10. Four-year (1987–1990) time series of monthly-averaged OGCM zonal velocity at 165°E on the equator.

Meridional Velocity in cm/s (OGCM Simulation)
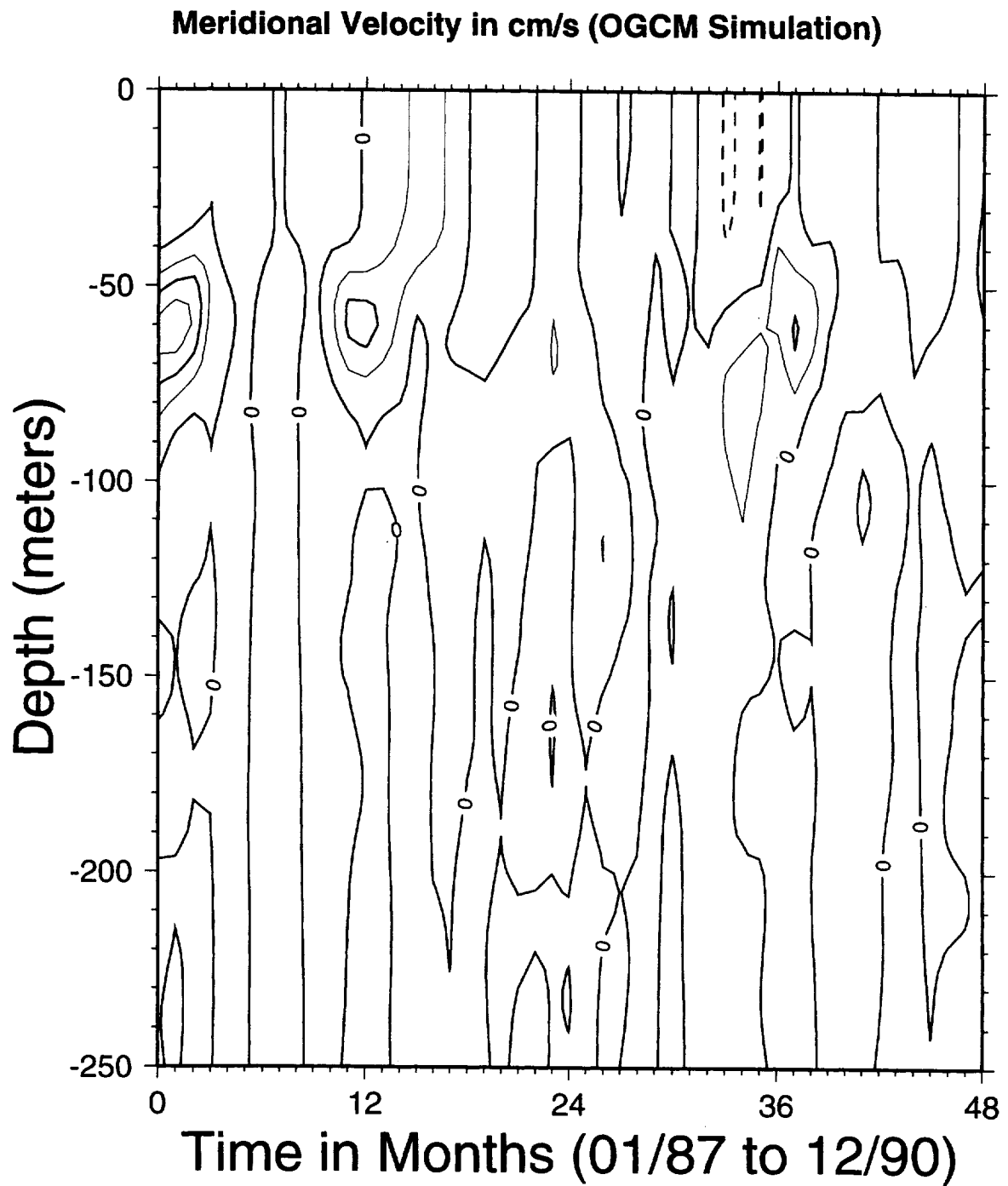
Figure 11. Four-year (1987–1990) time series of monthly-averaged OGCM meridional velocity at 165°E on the equator.
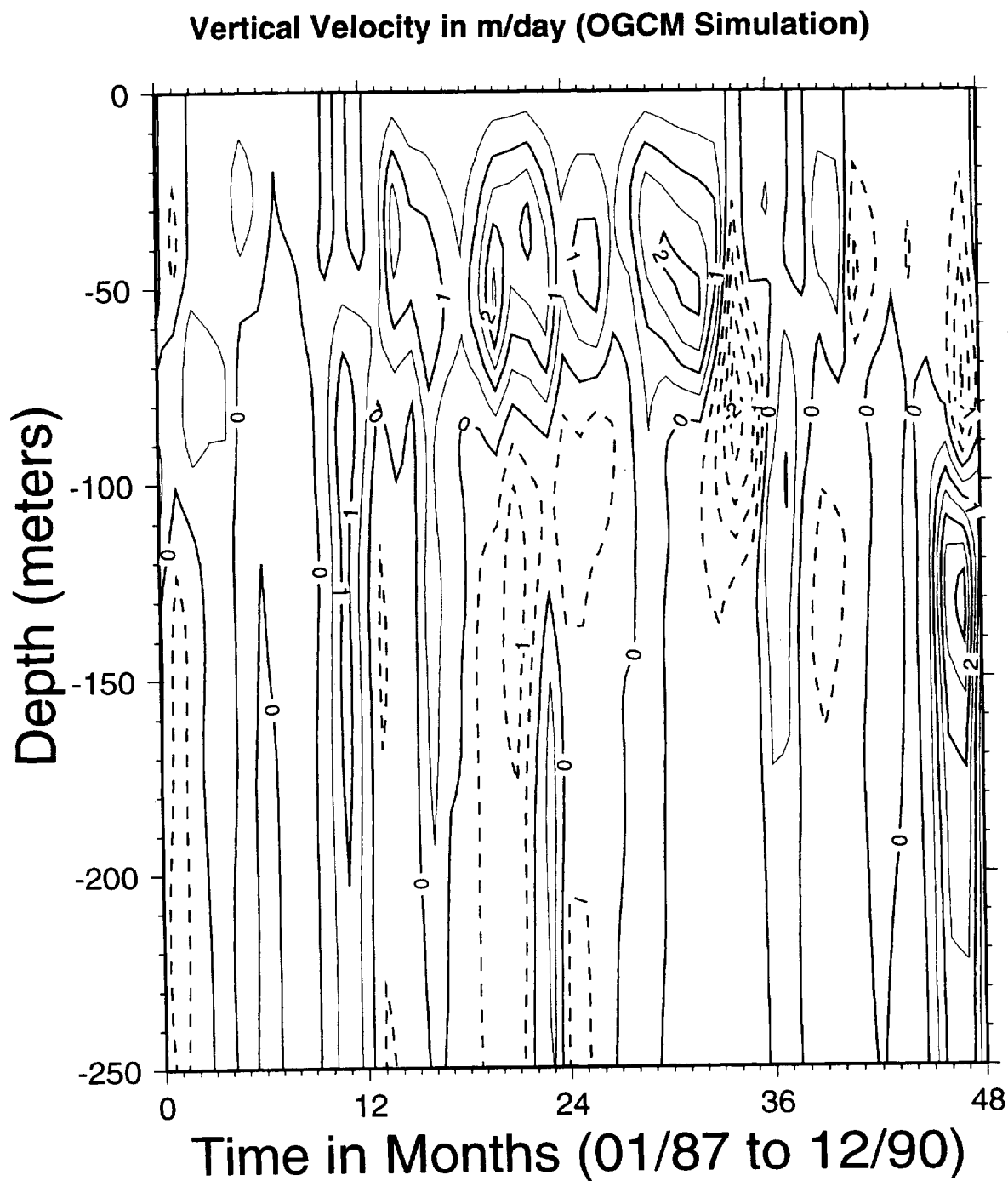
Figure 12. Four-year (1987–1990) time series of monthly-averaged OGCM vertical velocity at 165°E on the equator.

Temperature in °C (OGCM Simulation)
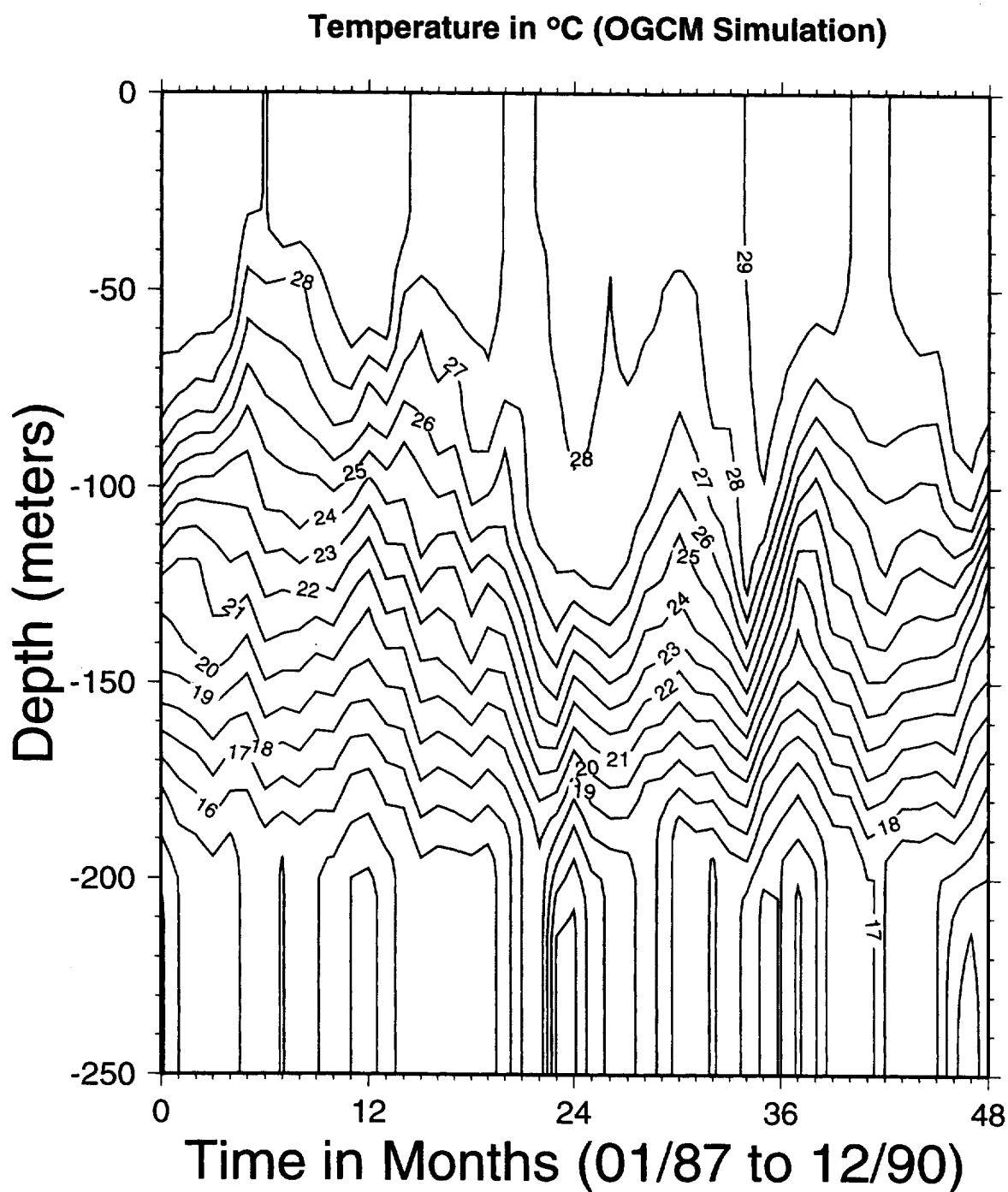
Figure 13. Four-year (1987–1990) time series of monthly-averaged OGCM temperature at 165°E on the equator.
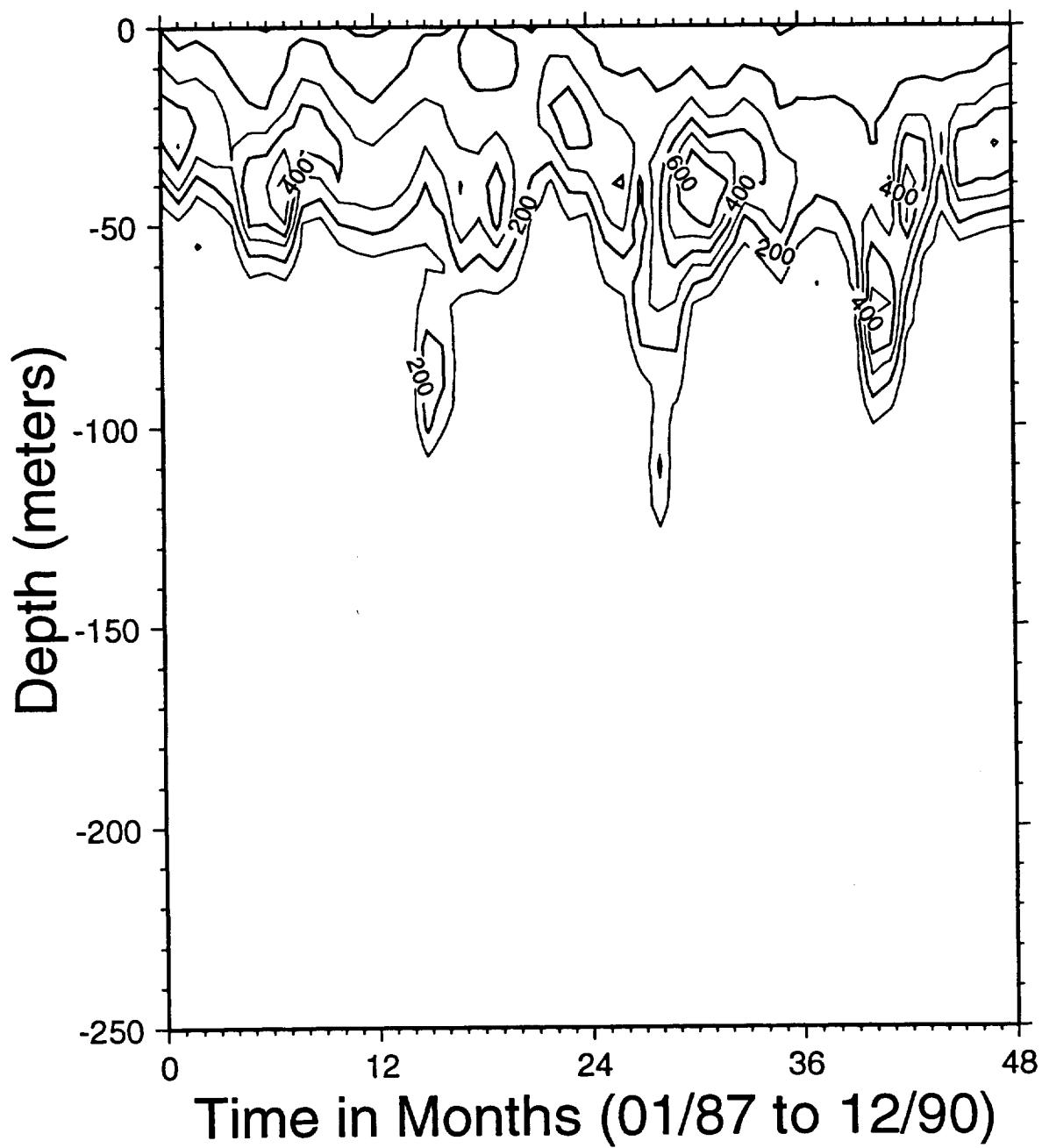
Figure 14. Four-year (1987–1990) time series of monthly-averaged vertical diffusivity (K_v) at 165°E on the equator. The values of K_v were calculated using the method of Pacanowski and Philander [1981] and physical fields simulated by the OGCM.

Meridional Velocity in cm/s (TOGA/TAO Data)
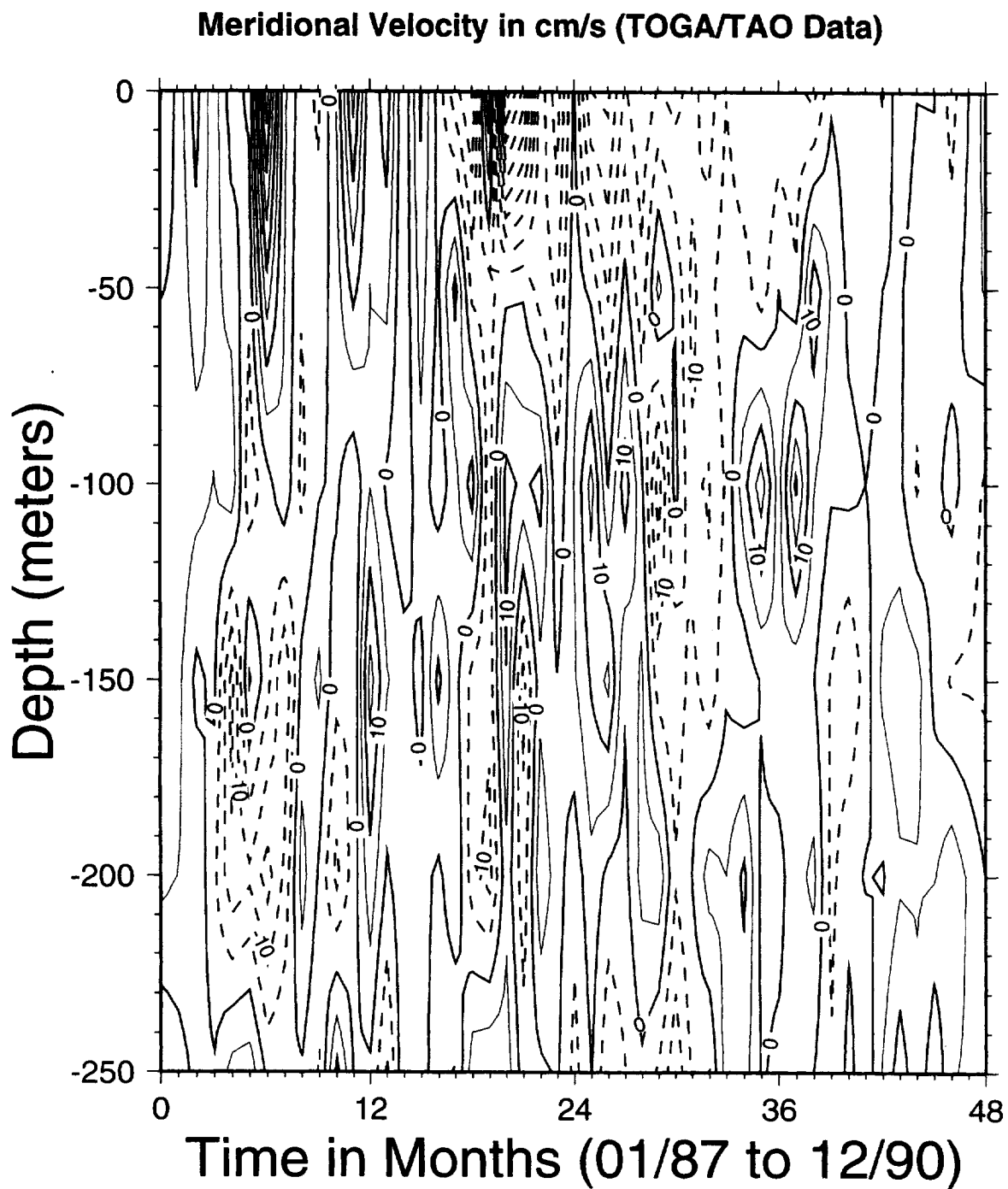
Figure 15. Four-year (1987–1990) time series of monthly-averaged TOGA–TAO meridional velocity at 165°E on the equator.

Zonal Velocity in cm/s (TOGA/TAO Data)
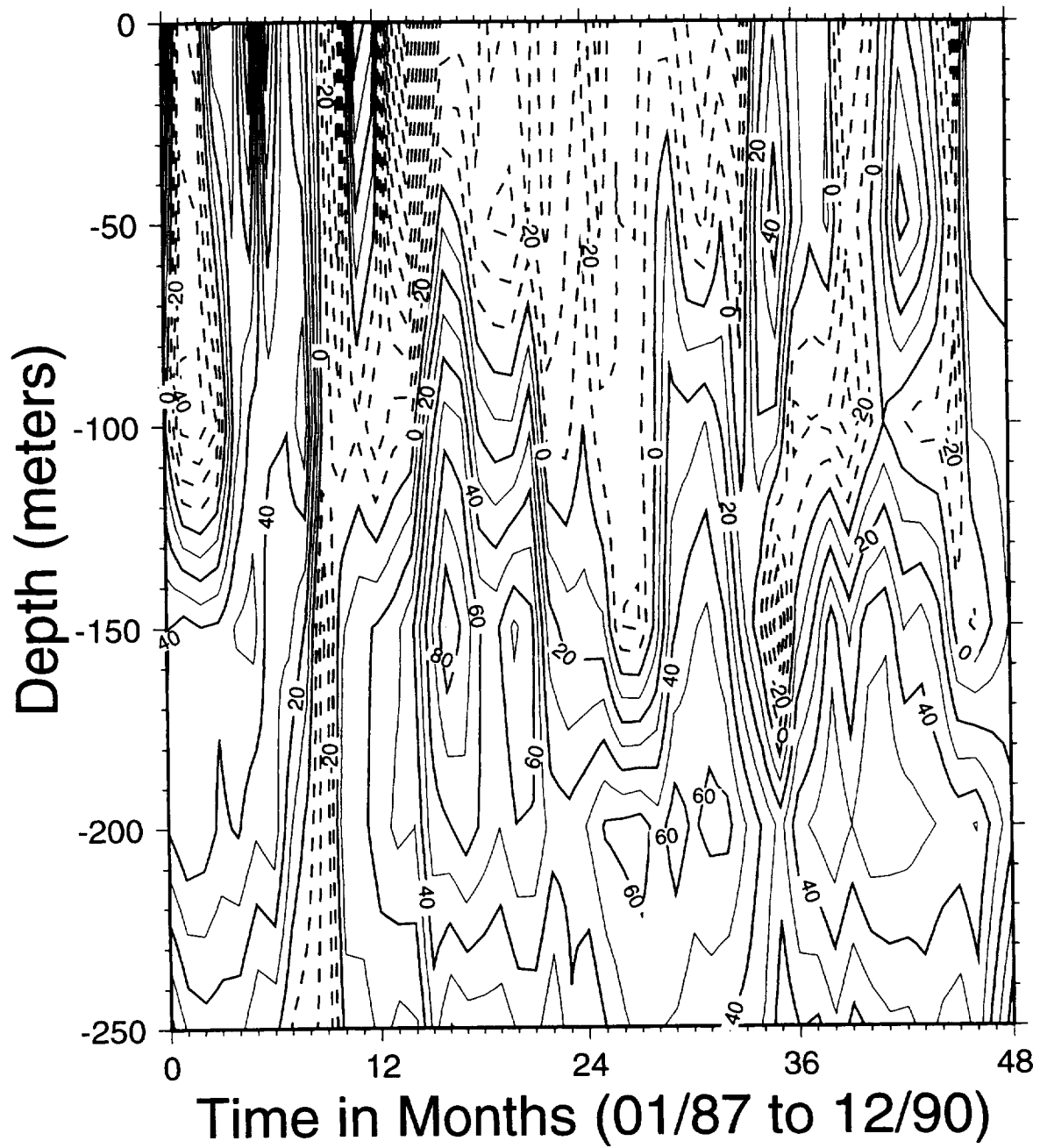
Figure 16. Four-year (1987–1990) time series of monthly-averaged TOGA–TAO zonal velocity at 165°E on the equator.
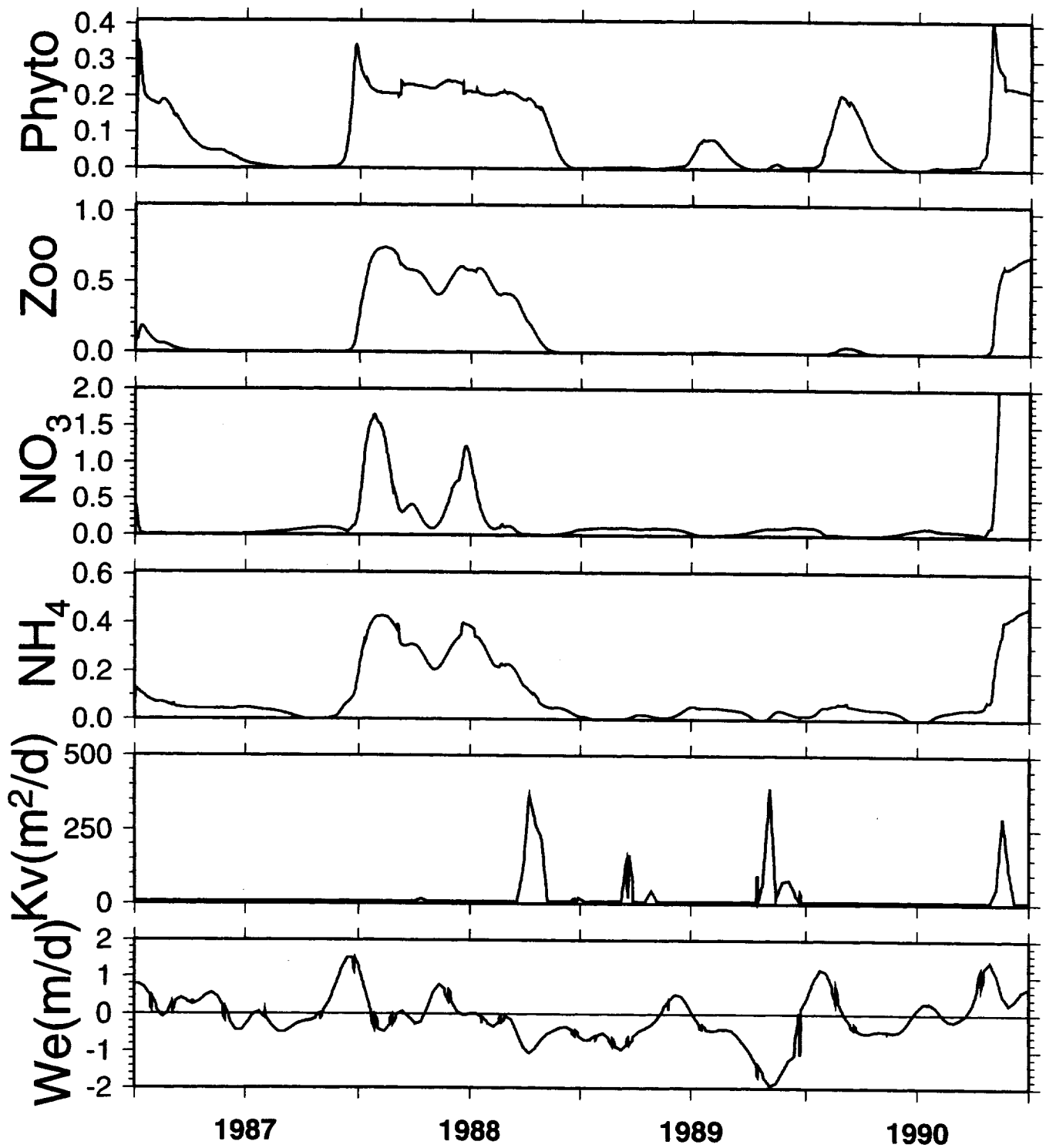
Figure 17. Composite four-year (1987–1990) time series of vertically averaged (0–50 m) phytoplankton, zooplankton, nitrate, and ammonium concentrations, combined with the vertical diffusivity and vertical velocity time series at 100 m originating from the OGCM-driven Warm Pool simulation.

TABLE 1

Ecological Model Variables and Input Parameter Definitions and Values. "Original" refers to the values used in McClain et al. (1996) and "spectral" are values tuned for effects of nitrification and remineralization.

| Symbol	OWS P (original)	OWS P (spectral)	Warm Pool	Definition
				Derived Quantities
P				Phytoplankton nitrogen, mg-at·N/m³
Z				Zooplankton nitrogen, mg-at·N/m³
NO_3				Nitrate, mg-at·N/m³
NH_3				Ammonium, mg-at·N/m³
G				Phytoplankton growth rate, 1/day
π_1				Regenerated production fraction
π_2				New production fraction
l				Zooplankton grazing rate, 1/day
				Initial Conditions
	0.2	0.2	0.1	Initial P concentration, mg-at·N/m³
	0.1	0.1	0.1	Initial Z concentration, mg-at·N/m³
	13.0	13.0	0	Initial surface nitrate concentration, mg-at·N/m³
	0.1	0.1	0.1	Initial ammonium concentration, mg-at·N/m³
				Phytoplankton Input Parameters
m	0	0.1	0.1	Death rate, 1/day
G_o	0.851	0.851	0.851	Growth rate at 0°C, 1/day
k_{gp}	0.0633	0.0633	0.0633	Temperature sensitivity of algal growth, 1/°C
η	0.02	0.02	0.02	Respiration coefficient
k_{rp}	0.0633	0.0633	0.0633	Temperature sensitivity of algal respiration, 1/°C
I_{kmax} (<60m)	25.0	25.0	400.0	Maximum photoacclimation parameter, μEin/m²/s
I_{kmax} (≥60m)	250.0	160.0	400.0	
K_{NO3}	1.0	1.0	1.0	Half saturation for nitrate uptake, mg-at·N/m³
K_{NH4}	0.1	0.1	0.5	Half saturation for ammonium up-take, mg-at·N/m³
pk	3.0	5.0	5.0	Ammonium inhibition of nitrate uptake, dimensionless
S_{max}	1.0	1.0	0	Maximum sinking rate, m/day
chla:N	1.0	1.0	1.0	Chlorophyll-a:Nitrogen ratio, mg/mg-at·N
				Zooplankton Input Parameters
g	0.04	0.1	0.04	Death rate, 1/day
R_m	5.0	4.75	7.0	Maximum grazing rate, 1/day
Λ	0.8	0.8	0.8	Ivlev constant, m³/mg-at·N
TH	0.0	5.0	0.0	Minimum C threshold for grazing, mgC/m³
γ	0.3	0.3	0.3	Unassimilated ingested ration, dimensionless
r_{zo}	0.019	0.019	(reformulated)	Respiration rate at 0°C, 1/day
k_{rz}	0.15	0.15	(reformulated)	Temperature sensitivity of respiration, 1/°C
				Nutrient Input Parameters
a_z	0.5	0.6	0.6	Fraction of dead zooplankton converted to ammonium
a_p	0.5	0.6	0.6	Fraction of dead phytoplankton converted to ammonium
A^n_{max}		2.0	2.0	Maximum rate of nitrification, nmol/day
D_{min}		0.0095	0.0095	Minimum irradiance (300-470 nm) for nitrification, W/m²
K_D		0.036	0.036	Half-saturation dosage for nitrification photoinhibition, W/m²/nm
C_{pel}		0.8	0.8	Fecal pellet remineralization fraction
				Physical Parameters
K_{Vbot}	17.3	17.3	8.65	Minimum (bottom) eddy diffusion coefficient, m²/day

APPENDIX A

The Interactive Data Analysis Package (IDAPAK)

IDAPAK is a software package designed at NASA GSFC to perform user-specific functions in connection with the preprocessing and analyses of geophysical data sets. IDAPAK was originally developed for personal computers (PCs) to complement PC-SEAPAK (Firestone et al., [1989]; Firestone et al., 1990; Darzi et al., [1991]), which did not support meteorological and hydrographic data analysis. Over the past few years, PC-IDAPAK has been ported to UNIX (Tai and McClain [1993]) where its functionality has been expanded by implementing the package under the commercially available Interactive Data Language (IDL) environment by Research Systems, Inc.

A.1 Hardware and Software Configurations

While most of IDAPAK programs are coded in FORTRAN-77 and C, the package makes extensive use of IDL, along with its graphical user interface (GUI), which is available for most UNIX systems. IDL is a powerful interpreter computer language which greatly expands the data analysis and display capabilities of IDAPAK. It provides many graphical and image display functions and also incorporates many data transformation and statistical application programs for image processing, data visualization, and scientific data analysis. The package can access data sets from a variety of sources and convert them into a simple columnwise ASCII format which is compatible with the other functions in the package and other PC and UNIX applications. All the input and output files in connection with ECO1D are in IDAPAK format.

A.2 Functions

The modules in IDAPAK are grouped into six different categories according to the characteristics of each module or program. They are:

- ACCESS (Data Access)
- PROCESS (Multivariable File Manipulation)
- ANALYSIS (Statistical Analysis and Derived Product Generation)
- MODEL (Oceanic Ecosystem and Radiative Transfer Models)
- DISPLAY (Data Display)
- ANIMATION (Data Animation)

Table A1 shows the current implementation of IDAPAK. Each module is an independent function. Most sources of meteorological and oceanographic data use different formats making the usage of the data and the development of application software more difficult. Olsen and McClain [1992] report on one effort to gather key oceanic data sets and archive them in a common format (the NASA Common Data Format, CDF) at the NASA Climate Data System (NCDS). This activity paralleled the development of the SEAPAK (McClain et al. [1992]) environmental applications module and interdisciplinary research using a variety of data sets (McClain et al., [1990]; Brock et al., [1991]; McClain and Firestone, [1993]) most of which were in CDF. NCDS has been phased out and support for many of the ocean data sets discontinued as NASA is now focused on the development of the EOS Distributed Active Archive Centers (DAACs).

Thus, most data sets presently being obtained are no longer in CDF, but are in the original formats. The programs under ACCESS reflect some of the more recent data sets used by the authors for ocean research.

The following subsections provide descriptions of each IDAPAK module.

A.2.1 ACCESS

The access programs decode data and convert them into an ASCII format designed for IDAPAK This ASCII format arranges data in column–row form with a small information header describing the number of columns, the format of each column and the content (variable descriptor) of each column. Data files with this format are transportable and easily edited. For example, they can be downloaded to a PC and processed using any other analysis or graphics software. The present suite of conversion programs can handle hydrographic station data from NOAA's NODC (National Oceanographic Data Center), data in netCDF (network Common Data Format), data from TOGA–TAO array, data generated by FOXPRO (a Microsoft database product) and several other data sets associated with specific field experiments or investigators. TOGA is an ongoing project for investigating the interactions between the tropical atmosphere and ocean. The TAO array of buoys are deployed across the tropical Pacific and some include solar irradiance measurements. TOGA–TAO data are either in ASCII or netCDF format. Once read by the ACCESS programs, the data can be processed, analyzed, and displayed using the other modules in IDAPAK. Table A2 describes each specific ACCESS function.

A.2.2 PROCESS

The PROCESS programs perform basic data and file manipulation operations such as copying, deleting, renaming, editing, cutting and pasting, listing, printing, merging, or appending different files into one file, reformatting, transposing, and chronological sorting. Table A3 describes each specific PROCESS function.

A.2.3 ANALYSIS

The programs for basic statistical analysis such as auto- and cross-correlation, linear regression, fast Fourier transformation, and maximum entropy spectral analysis are collected under the ANALYSIS module. There are also functions for smoothing, interpolation using different algorithms (linear and cubic spline), and simple columnwise algebraic operations for multi-variable files. Table A4 describes each specific ANALYSIS function.

A.2.4 MODEL

The **MODEL** module incorporates a variety of analytical and numerical model products. **DERIVED_V** is a program that computes 20 meteorological and oceanographic derived quantities from basic input (see Table A5).

SOLAR_G&C, a solar irradiance model by Gregg and Carder [1990], estimates the clear sky surface spectral downwelling solar irradiance at 1 nm resolution from 350 to 700 nm. **SOLAR_F** (Frouin et al., [1989]), estimates broad-band clear sky solar irradiance for 250–4000 nm, 350–700 nm and 400–700 nm. **SOLAR_G** computes the total clear-sky solar irradiance (Garwood, personal communication).

COUPLED_M includes 3 one-dimensional marine ecosystem models which differ mostly in the way that the physical parameters are calculated. The first one couples mixed layer dynamics [Garwood, 1977], biological processes [McClain et al., 1996] and the surface irradiance models (Frouin et al., [1989]; Gregg and Carder, [1990]) . The model is driven by surface meteorological variables (wind speed, cloud cover, air temperature, and dew point temperature). These variables are used to determine the surface latent, sensible, short wave and long wave heat fluxes, and the wind stress. The subsurface light field is determined using the vertical profile of chlorophyll as estimated from the biological model.

Table A1. IDAPAK programs listed by program category.

ACCESS	PROCESS	ANALYSIS	MODEL	DISPLAY	ANIMATION
ARRIGO	ADDJULIAN	AREAVGIDA	DERIVED_V	SET_WINDOW	NODC_PROF
BISHOP_PAR	APPEND	AVERAGING	COUPLED_M	INSIGHT	IDA_LINE
BRS_CDF	BOUND	AVG_FILES	SOLAR_G&C	CREATE_MAP	IDA_PROF
BRS_DAAC	CONV_FMT	BANDPASS	SOLAR_F	VIEW_CZCS	CZCS
BRS_HDF	COPY	BINNING	SOLAR_G	VIEW_HDF8	HDF8
BRS_NETCDF	DEL_ROW	COLUMNOPER		VIEW_HDF24	HDF24
CDFLST2IDA	EDIT	CORRELATION		VIEW_SFC	DAAC_BINARY
CREATE	IMAGE	FFTIDA		VIEW_PROF	SUE_BINARY
ENV_QUERY	INSERT_COL	FUNCSIDA		VIEW_LINES	
EXCEL2IDA	LIST	GETIDAMLD		PLOT_CONTRS	
FOXPRO	MERGE	INTEGRATION		PLOT_SFC	
FRENCH	RANGE	INTERPOLA		PLOT_LINE	
GARWOOD	REFORMAT	MEMSPCIDA		PLOT_PROF	
GETCDF	REMOVE	REGRESSION		PLOT_SCATTR	
GETDAAC	RENAME	SMOOTH		SURF_CONT	
GETIDLBIN	RM_9999	SPLINE		TRACKING	
GETISCCP	PAGECUT	STDEV		TOGA_CROSS	
GETNODC	PRINT	SUMCOL		VECTOR_PLOT	
GETRAGU	SAMPLE	SUMIDA			
GETSALT	SELECT				
GETSUE	SORTING				
GETWOA	STRIPHDR				
TAO_RAD	TRANSPOSE				
TAO_RAD_20					
TOGA_TAO					
TIMENV2IDA					

Table A2. Description of IDAPAK ACCESS functions.

ARRIGO	Data Formatted by K. Arrigo (NASA/GSFC)
BISHOP_PAR	Data Archived by J. Bishop in HDF SD format
BRS_CDF	NASA CDF browse data
BRS_DAAC	DAAC binary browse data
BRS_NETCDF	netCDF browse data
BRS_HDF	HDF browse data or images, and entire array dump
CDFLST2IDA	Converts CDFLIST ASCII data to IDA format
CREATE	Creates data using NEDIT
ENV_QUERY	Inquires CDF data sets stored in OCF at NASA/GSFC
EXCEL2IDA	Converts from Microsoft Excel CSV ASCII data to IDA format
FOXPRO	Extracts data generated by FOXPRO
GARWOOD	Data formatted by R. Garwood
FRENCH	Reads data generated by French research ships
GETCDF	Extracts data from two-dimensional CDF ASCII data sets
GETDAAC	Extracts data from DAAC binary files or IDL binary files
GETIDLBIN	Extracts IDL binary data and converts to 2D CDF ASCII or row/column format
GETISCCP	Converts NASA/Langley ISCCP HDF data to CDF 2D ASCII or row-column formats
GETNODC	Extracts NODC data from optical disk or CD-ROM
GETRAGU	Extracts OGCM data generated by R. Murtuggude
GETSALT	Extracts salinity profile data and converts it to ASCII column format
GETSUE	Extracts SUE surface flux data
GETWOA	Extracts CD-ROM data archived by WOA
TOGA_TAO	Extracts TOGA-TAO meteorological data formatted in netCDF or ASCII
TAO_RAD	Extracts irradiance data archived from TAO buoys
TAO_RAD_20	Averages 20-minute irradiance data from TAO buoys to hourly data
TIMEN2IDA	Converts SEAPAK TIMENV ASCII data to IDL

Table A3. Description of IDAPAK PROCESS functions.

ADDJULIAN	Adds Julian date to an IDAPAK file
APPEND	Appends IDAPAK files into a single file
BOUND	Allows user to specify high and low acceptance bounds for variables in the data file
CONV_FMT	Converts IDAPAK, CZCS, and CDF files into other formats (ASCII, CZCS, and CDF)
COPY	Copies one IDAPAK file into another
DEL_ROW	Deletes rows from IDAPAK files (start/stop dates must be specified)
EDIT	Allows user to edit files on an IDAPAK window
IMAGE	Image processor (composites, convertions,histograms, median and filters)
INSERT_COL	Inserts columns into an IDAPAK file
LIST	Lists files on an IDAPAK window (general, IDAPAK, and NODC formats)
MERGE	Merges the data columns of IDAPAK and ASCII files into a single file
RANGE	Disabled
REFORMAT	Converts IDAPAK files from floating to exponential formats, and vice-versa
REMOVE	Deletes a file
RENAME	Renames a file
RM_9999	Remove record nulls from a file
PAGECUT	Allows user to extract a subset of variables from a file
PRINT	Prints a file
SAMPLE	Sub-samples an IDAPAK or NODC file according to time and geographic bounds
SELECT	Selects data from a file based on station ID, date and hour, and prints to another file
SORTING	Sorts IDAPAK time series and profile data into yearly, monthly, and seasonal time bins
STRIPHDR	Strips the header information from IDAPAK or ASCII files
TRANSPOSE	Transposes rows and columns in a file and prints results to another file

Table A4. Description of IDAPAK ANALYSIS functions.

AREAVGIDA	Computes area-averaged values from a file given geographical boundaries
AVERAGING	Computes total,yearly,monthly,daily,12-,6-,3-hourly, and hourly time averages
AVG_FILES	Combines any number of specified files and averages them into a single file
BANDPASS	Applies a bandpass filter to variables in a file given the lower and high frequencies
BINNING	Bins the data in a file according to monthly, seasonal or total means
COLUMNOPER	Applies user-specified operators +, -, x, and / to individual columns in a file
CORRELATION	Calculates the cross-correlation between variables within a file or in separate files
FFTIDA	Applies a Fast Fourier Transform (FFT) to specific variables in a file
FUNCSIDA	Applies arithmetic, logarithmic, and trigonometric operators to columns in a file
GETIDAMLD	Gets mixed-layer depth from a temp record using Levitus or buoyancy methods
INTEGRATION	Reads vertical profiles and averages, integrates, and picks values from given levels
INTERPOLA	Interpolates time series and profiles at given intervals of time or depth
MEMSPCIDA	Performs spectral analysis given filter and bandwidth specifications
REGRESSION	Linear regression between two variables within a file or separate files
SMOOTH	Filters specific data sets within a file given filter characteristics
SPLINE	Fits a spline into vertical profiles or time series given the spline and data specs
STDEV	Calculates max, min, sum, mean, and std deviation of all columns in a file
SUMCOL	Sums and multiplies data columns in a file given a specific operator
SUMIDA	Time series sum (as in AVERAGING, except that it is not divided by no. of points)

Table A5. List of quantities that can be computed in IDAPAK given the required input fields.

1. Water density	22. Longwave radiation (Garwood for clear sky)
2. Dew point temperature	23. Longwave radiation (Berliand and Berliand, [1952])
3. Vapor pressure	24. Longwave radiation (Budyko, [1963])
4. Relative humidity	25. Longwave radiation (Budyko, [1963])(Clear sky)
5. Mixing ratio	26. Surface irradiance (Budyko, [1963])
6. Potential temperature	27. Surface irradiance (Reed, [1977])
7. Equivalent potential temperature	28. Surface irradiance (Dobson & Smith, [1988])
8. Zonal & meridional wind components	29. Clear sky surface irradiance (ocean) (Davis)
9. Zonal & meridional wind stress ($_{x, y}$)	30. Clear sky surface irradiance (ocean) (Atwater)
10. Total wind stress (τ)	31. Clear sky surface irradiance (land)(Davis)
11. $\tau^{3/2}$	32. Clear sky surface irradiance (land) (Atwater)
12. Zonal & meridional Ekman transport	33. Visibility (km)
13. Total Ekman transport	34. Water content (cm)
14. Ekman depth	35. Albedo
15. Sensible heat flux (SH)	36. Solar zenith angle
16. Latent heat flux (LH) (4 inputs)	37. Cosine of zenith angle
17. Latent heat flux (LH) (5 inputs)	38. Solar altitude
18. Bulk coefficient for SH	39. Julian date
19. Bulk coefficient for LE	40. Clear sky surface irradiance (Ocean) (Frouin)
20. Longwave radiation (Garwood, 3 input values)	41. Clear sky surface irradiance (Land) (Frouin)
21. Longwave radiation (Garwood, 4 input values)	

The second model is similar to the first model, except that the mixed layer dynamics are simulated by the Chen et al. [1994] one-dimensional model. As mentioned in Sections 1.3 and 1.4, the mixed layer model of Chen et al. [1994] was modified by adding flux and diffusion adjustment terms for preventing excess heating at the bottom of the model domain, which propagates upward to the surface. Besides this modification, biological processes are reformulated to include nitrification of ammonium and remineralization of fecal pellet production. The vertical velocity field is either derived from the ocean model (Murtugudde et al, [1996]) or calculated from an empirical formula (McClain and Firestone [1993]). The algorithm for the estimation of diffusivity in the water column uses the method of Pacanowski and Philander [1981]. This method requires current velocity and potential temperature. The TAO buoys deployment over the tropical Pacific provide daily records of these variables; however, the temporal data set coverage is very limited. To have a longer period of simulation, the model was upgraded into a third version that allows the ingestion of profiles of current, temperature, and vertical velocity computed by the OGCM (Murtuggude et al., [1994]). All these models generate time series and profiles of different variables for diagnostics and analysis purposes. Tables A6, A7, A8, A9, and A10 show examples of model output stored on five different output files that can be viewed and analyzed with the IDAPAK Graphic User Interface (GUI) functions described in Section A.2. These files can be easily modified in the corresponding FORTRAN modules to satisfy specific user needs and future model upgrades.

Table A6. Time series of diagnostic and predicted variables (file 'namef.asc' in Section B2.2)

1. Mixed layer depth	14. Zooplankton
2. Predicted sea surface temperature	15. Ammonium
3. Observed sea surface temperature	16. Nitrate
4. Air temperature	17. Radiation at surface
5. Salinity	18. Radiation at mixed layer
6. Q (sensible heat)	19. Averaged mixed layer depth
7. Q (longwave radiation)	20. Gross production
8. Q (latent heat)	21. Net production
9. Q (radiation just below surface)	22. New production
10.Q (radiation of clear sky)	23. F ratio
11. Q (radiation at surface)	24. Radiation at mixed layer of OGCM
12. Radiation at mixed layer depth	25. Mixed layer depth of OGCM
13. Phytoplankton	26. PAR at surface

Table A7. List of variables in the output file containing vertical profiles generated by the coupled model (file 'namep.asc' in Section B2.2).

1. Depth	13. Vertical Diffusivity
2. Julian date	14. Phytoplankton Respiration rate
3. Temperature	15. Vertical velocity
4. Salinity	16. C:Chla
5. Phytoplankton	17. Zooplankton respiration rate
6. Zooplankton	18. 24-hour running mean of subsurface light (E^*)
7. Ammonium	19. Llim
8. Nitrate	20. Nlim
9. 24-hour averaged growth rate	21. Beta term
10. Grazing rate	22. NO_3_lim
11. F ratio	23. NH_4_lim
12. Profile of PAR	24. Integrated daily gross production

Table A8. List of variables in the output file containing the time series of integrated data (file 'namet.asc' in Section B2.2).

1. Phytoplanton integrated to 50 m	16. F ratio for column
2. Zooplankton integrated to 50 m	17. Sensible heat flux
3. Ammonium integrated to 50 m	18. Heat flux due to back radiation (longwave)
4. Nitrate integrated to 50 m	19. Latent heat flux
5. Phytoplankton integrated for column	20. Clear sky total radiation just above the surf.
6. Zooplankton integrated for column	21. Cloudy sky total radiation just above the surf.
7. Ammonium integrated for column	22. Cloudy sky total radiation just below the surf
8. Nitrate integrated for column	23. Gregg-Carder PAR just below the surface
9. Gross production for 50 m	24. Gregg-Carder PAR at the mixed-layer depth
10. Net production for 50 m	25. Frouin clear-sky PAR just above the surface
11. New production for 50 m	26. Frouin clear-sky PAR just below the surface
12. Gross production for column	27. Frouin cloudy-sky PAR just above the surface
13. Net production for column	28. Frouin cloudy-sky PAR just below the surface
14. New production for column	29. Dobson clear sky radiation
15. F ratio for 50 m	

Table A9. More time series of predicted and diagnostic model variables (file 'namen.asc' in Section B2.2).

1. Mass loss due to grazing	10. Observed temperature at 250 m
2. Column-integrated pct of Phyto transformed into ammonium	11. Predicted temperature at 250 m
3. Column-integrated pct of Zoo transformed into ammonium	12. Ratio of light penetration to total surface irradiance (γ)
4. Nitrate concentration at the bottom	13. Avg growth within euphotic zone
5. Vertical advection of NO_3 at the bottom	14. Avg Phyto within euphotic zone
6. Sinking rate of Phyto at the bottom	15. Avg NO_3 within the top 5 depths
7. Total mass at each time step (Phyto+Zoo+ NO_3+NH_4)	16 Avg NO_3 between 56–65 m.
8. Total mass change at each time step	17. Frouin to Gregg-Carder PAR ratio
9. Total mass loss at the bottom	

All the models and formulas need initial input data of various kinds. This information is passed to the model or formulas through the GUI. The input data and results from these models are all preprocessed using other IDAPAK modules. Post-processing and display of model outputs are also accomplished using IDAPAK modules. The user may access data from different data sources and generate the inputs required by the models using programs in PROCESS and ANALYSIS modules. The results of models may be displayed or animated by functions in DISPLAY and ANIMATION.

A.2.5 DISPLAY and ANIMATION

DISPLAY and ANIMATION have functions for displaying and animating the column–row formatted data and image files. Since IDL provides a very comprehensive graphical display and image processing library, all the programs in these two modules are coded in IDL. The display module allows the user to display one-dimensional time series data, contour two-dimensional fields, and annotate graphs interactively. For irregularly distributed horizontal data, the user can generate contours on a variety of map projections. All

DISPLAY programs allow the user to generate PostScript™ output. The ANIMATION programs support looping ASCII profile data and CZCS image files.

Table A10. Diagnostic file containing daily profiles of all phytoplankton, zooplankton, nitrate and ammonium terms in (41) through (44) (file 'diag_bal_name.dat' in Section B2.2).

1. Depth	16. NO_3 time change ($\partial NO_3/\partial t$)
2. Phyto time change ($\partial P/\partial t$)	17. NO_3 vertical advection ($w\partial NO_3/\partial z$)
3. Phyto vertical advection ($w\partial P/\partial z$)	18. NO_3 vertical diffusion ($k_v\partial^2 NO_3/\partial z^2$)
4. Phyto sinking rate ($\partial SP/\partial z$)	19. NO_3 uptake by phytoplankton ($\pi_2 GP$)
5. Phyto vertical diffusion ($k_v\partial^2 P/\partial z^2$)	20. Ammonium nitrification (A_n)
6. Phyto growth rate (GP)	21. NH_4 time change ($\partial NH_4/\partial t$)
7. Phyto mortality rate (mP)	22. NH_4 vertical advection ($w\partial NH_4/\partial z$)
8. Phyto respiration rate ($r_p P$)	23. NH_4 vertical diffusion ($k_v\partial^2 NH_4/\partial z^2$)
9. Zoo grazing on Phyto (IZ)	24. NH_4 production from phyto mortality ($a_p mP$)
10. Zoo time change ($\partial Z/\partial t$)	25 NH_4 production from phyto respiration ($r_p P$)
11. Zoo vertical advection ($w\partial Z/\partial z$)	26. NH_4 loss due to phyto growth ($-\pi_1 GP$)
12. Zoo vertical diffusion ($k_v\partial^2 Z/\partial z^2$)	27. NH_4 production from zoo mortality ($a_z gZ$)
13. Zoo growth ($[1-\gamma]IZ$)	28. NH_4 production from zoo respiration ($r_z Z$)
14. Zoo death rate (gZ)	29. NH_4 production from zoo fecal pellets ($c_{pel}\gamma IZ$)
15. Zoo respiration rate ($r_z Z$)	30 NH_4 loss due to nitrification ($-A_n$)

APPENDIX B

Model Configuration and FORTRAN Routine Modules Used by the One-Dimensional Ecological Model (ECO1D)

This appendix provides descriptions of the model configuration and FORTRAN routine modules used by two versions of the ecosystem model. Version 1 consists of a coupled Garwood [1977] MLM with the spectral version of the 4-component ecosystem model. Version 2 uses the same 4-component ecosystem model but the physical forcing fields (u,v,w,T) are either derived from observations (e.g., TOGA–TAO array) or from an independently run OGCM. Since both versions share the same bio-optical algorithms, a certain degree of overlap in the descriptions of the two model versions is inevitable. The following sections address details of model configuration and usage.

B.1   ECO1D with Garwood MLM Coupling

This section describes the input parameters, nominal values, input and output files, program flowchart, and FORTRAN routine names and functions for the ecosystem model using the Garwood [1977] MLM.

B.1.1 Input Parameters and Nominal Values

The input parameters and nominal values used by the ecosystem model are read in from a file (filename.par) specified in the command line when executing the model run:

% eco1d < filename.par &

The initial and forcing fields required for the multi–year runs are read in from other files specified in Section B1.2. The format for all parameters in 'filename.par' is provided in the main FORTRAN module 'opblpc.f'. The following table summarizes each of the input parameters contained in the file.

IC=	Types of initial temperature (T) and salinity (S) profiles
	-1: use default $T(z)$ and $S(z)$
	0: use analytic $T(z)$ and default $S(z)$
	1: use Garwood $T(z)$ and default $S(z)$
	2: user's provided $T(z)$ and default $S(z)$
	3: user's provided $T(z)$ and $S(z)$
	4: use $T(z)$ and $S(z)$ produced in last run
IB=	Boundary condition source
	0: analytical forcing test case for MLM
	1: read boundary values from external sources
IE=	Upwelling option:
	0: use constant vertical velocity We
	1: evoke Ekman upwelling calculation
CB=	Biological model option:
	0: no biological model evoked
	1: couple mixed layer model with biological model
FB=	Switch to enable bio-absorption of light

| | 0: no |
| | 1: yes |

IP=	Switch for initial nutrient concentration file:
	1: use default values
	2: read initial nitrate and ammonium concentrations from units 7,8
	3: read initial nitrate and ammonium concentrations from hot start file (7)
	4: read initial nitrate concentration from unit 7 and use default ammonium values

DD=	Switch to print results:
	0: do not print results
	1: print results

DB=	Switch to print daily-averaged time series of surface and depth-averaged values:
	0: do not print time series
	1: print time series

CV=	Switch to control writing of hot start file:
	0: do not write hot start file
	1: write hot start file

HR = 24	Controls frequency (in hours) of output of model variables (except for profiles)
HP = 24	Controls frequency (in hours) of output of vertical profiles
v= 2.79	Atmospheric water content (cm)
uo= 0.34	Ozone concentration (Doobson)

a_type=	Aerosol type:
	0: Continental
	1: Oceanic

Cldbb=0.50	Cloud correction coefficient
Cldaa=0.53	Cloud correction coefficient
shift=5.0	Shift angle (degrees) for the periodic seasonal cloud effect
dt=0.3600D+04	Model time step (seconds)
dz =0.1000D+01	Vertical grid resolution (meters)
phs= 0.0	Phase for analytical vertical motion parameters
per= 365	Period for analytical vertical motion parameters
A75= 0	Internal wave amplitude at 75 meters

NST=	Controls equation of state
	0: constant thermal expansion coefficient
	1: uses temperature-dependent thermal expansion coefficient

| AT= 0.02 | Diffusion coefficient at the top of the mixed layer (in cm^2/s) |
| AB= 0.02 | Diffusion coefficient at the bottom of the mixed layer (in cm^2/s) |

NV=	Switch to control diffusion in MLM
	1: temperature diffusion only
	4: diffusion of all variables

| H=350.0 | Maximum depth for model calculations |
| P1= 1 | Coefficient for ML entrainment equation |

P2= 1	Coefficient for ML entrainment equation
P3= 1	Coefficient for ML entrainment equation
M3 = 0.5	Coefficient for heat flux equation
K= 0.004	Extinction coefficient
AKD=0.0525	Coefficient for the vertical profile of diffusion used by the bio model
ZONE=25.0	Depth of transition layer (meters)
BOTKV=8.65	Minimum vertical diffusivity (Kv in m^2/day)
Mlcr=1	Controls number of variables to be printed (set to 12)
Mlv= 0.1	Criterion coefficient to find mixed-layer depth
Mcr= 30	Minimum mixed-layer depth in meters
We= 0.25	Upwelling velocity (m/day)
LAT= 50.0	Latitude in degrees (North is positive)
LON= -145.0	Longitude in degrees (East is positive)

IW=	Control for upwelling velocity:
	1: constant We
	2: read in We from external source

m= 0.1	Phytoplankton death rate, d^{-1}
G0= .8511	Phytoplankton growth rate at $0^{\circ}C$, d^{-1}
Kno3= 1.0000	Half saturation of nitrate uptake, mg-at N m^{-3}
Knh4= .5000	Half saturation of ammonium uptake, mg-at N m^{-3}
c= 0.02	Ratio of phytoplankton respiration to growth
Ideep = 25.0	Maximum photoacclimation parameter ($\geq$ 60 m), μmol quanta/m^2/s
Ishal= 160.0	Maximum photoacclimation parameter (< 60 m), μmol quanta/m^2/s
mixed= 60.0	Critical depth (meters) for Ishal and Ideep calculation
NH4= 0.1	Default initial NH4 value (if input file not assigned)
NO3= 13.0	Default initial NO3 value (if input file not assigned)
P = 0.2	Initial Phytoplankton concentration, mg-at N m^{-3}
Z = 0.1	Initial Zooplankton concentration, mg-at N m^{-3}
pk= 5.0	Nitrate-sensitive coefficient due to ammonium
Knir= 2.5	Attenuation coefficient for Near Infrared (m^{-1})
K_V = 1.0	Minimum value for K_V (m^2/d)
CHLN= 1.0	Chlorophyll-a:Nitrogen ratio, mg/mg-at N
DI = 2	Index to control the method to compute surface diffusivity
cs= 2	Index for choosing the method to compute the diffusivity profile
fc=1.0	Multiplicative factor to apply to vertical diffusivity
Smax= 1.0	Sinking speed (m/d)
g= 0.1	Zooplankton death rate, d^{-1}
Rm= 4.75	Zooplankton maximum grazing rate, d^{-1}
LAMBDA= 0.8	Ivlev constant, m^3/mg-at N
GAMMA= 0.3	Unassimilated zooplankton ingested ratio, dimensionless
rz0= 0.0190	Not used - reformulated
krz= 0.15	Temperature sensitivity of zooplankton respiration, $^{\circ}C^{-1}$
Znh4 = 0.6	Fraction of dead zooplankton converted to ammonium
Pnh4 = 0.6	Fraction of dead phytoplankton converted to ammonium
TH = 5.0	Minimum C threshold for zooplankton grazing, mgC/m^3
MOVING= 24	Moving average window in hours for light energy
START= 19510101	Starting date for calculations, year/month/day
NDAYS=10957	Total number of days of simulation

IMLD= 1	Switch for depth integration limits (T1)
	1: surface to mixed-layer depth
	2: surface to bottom

T2= 50.0	Integration depth limits (meters)
T3= 350.0	Integration depth limits (meters)
DLEVEL= 350.0	Maximum depth level for model output (meters)
INTV= 10.0	Depth interval for output (meters)
BLKCH=0.0015	Transfer coefficient for sensible heat flux
BLKCE=0.0015	Transfer coefficient for latent heat flux
NDG=2	Controls calculation of drag coefficient for wind stress
NFX=1	Controls calculation of heat flux transfer coefficient

NLW=1   Switch to control longwave radiation scheme
                                   1: Tseng method (W/m^2)
                                   2: Budyko method $(Kcal/cm^2/month)$

NH4OX=2.0	Maximum rate of nitrification (nmol/day) ·
HALF=0.036	Half-saturation dosage for nitrification photoinhibition $(W/m^2/nm)$
ZtoNH4=0.8	Remineralization coefficient for fecal pellets
CLDF=1.0	Multiplicative factor to apply to cloud cover
CLC=0.001289	Cloud cover coefficient

DRAG=1   Controls drag coefficient scheme
                                   1: Amorocho and Devries
                                   2: Constant coefficients

YR=1951	Beginning year
JULIAN=1	Beginning Julian day

B.1.2 Input and Output Files

The following logic units (LU) and input/output file names are specified in 'filename.par' after the last parameter input described in section B1.1. The file names and data sets that they contain are only given as examples; other data sets for different time periods and geographical areas can be specified by the user. Note that LU=TMP means temporary logic unit.

Logic units (LU) for input/output files

1 2 3 11 12 13 14 7 8

Input files

/user_pathname/xbt250.dat	LU=01;	Initial temperature profiles from XBTs
/user_pathname/papa5181.dat	LU=02;	Environmental data from OWSP (1951-1981)
/user_pathname/ekman1.dat	LU=03;	Pre-calculated Ekman vertical velocities (w_e)

Output Files

/user_pathname/namef.asc	LU=11;	Daily time series of selected diagnostic and predicted model variables (see Table A6)

/user_pathname/namep.asc	LU=12;	Daily time series of vertical profiles for selected model variables (see Table A7)
/user_pathname/namet.asc	LU=13;	Daily time series of column-averaged and surface values for selected model variables (see Table A8)
/user_pathname/namen.asc	LU=14;	More daily time series of selected diagnostic and predicted model variables (see Table A9)

Input files

| /user_pathname/decno350.dat | LU=07; | Climatological nitrate (NO_3) concentration profile |
| /user_pathname/winnh4.dat | LU=08; | Climatological ammonium (NH_4) concentration profile |

Output Files

| /user_pathname/lastdyn.bin | LU=TMP; | Binary file containing dynamic variables from last time step to be used for hot starting the model |
| /user_pathname/lastbio.bin | LU=TMP; | Binary file containing biological variables from last time step to be used for hot starting the model |

Input files

/user_pathname/uvatmodd.dat	LU=TMP;	Spectral absorption coefficients for Gregg-Carder model
/user_pathname/wv_chl_absp.dat	LU=TMP;	Attenuation coefficients due to chlorophyll
/user_pathname/asnh4.dat	LU=TMP;	Ammonium nitrification coefficients

B.1.3 Ecosystem Model Flowchart

Figure B1.1 shows a flowchart for the first version of the ecosystem model, which consists of a one-dimensional MLM (Garwood, [1977]) coupled with the 4-component biological model. The flowchart identifies each main FORTRAN module in a separate box, with the arrows indicating input/output data flows and time stepping loops.

START

READ INPUT
PARAMETERS

READ WATER
ABSORPTION
COEFF. FOR NH4

CALL DAYTIM
COMPUTE FIRST
JULIAN DAY FOR
COMPUTATION

CALL ICOND
READ INITIAL
CONDITIONS
FOR T(z), S(z)

CALL ABSRP1
INTEGRATE Qs
AND ADJUST T(z)
FOR
UNDERWATER
ABSORPTION

CALL RETR
COMPUTE
INITIAL ML
RETREAT

CALL PSTAR
COMPUTE
INITIAL NON-
DIMENSIONAL
ENTRAINMENT

CALL BSMN
COMPUTE
INITIAL CRITICAL
VALUE OF
BUOYANCY

CALL DIFF
CALL GARDIFF
COMPUTE DIFFUSION
BELOW MIXED-LAYER

CALL LEVMLD
COMPUTE MIXED
LAYER DEPTH

CALL INITPZN
INITIALIZE
BIOLOGICAL
FIELDS

CALL PROFHEADS
CALL WTZPROFS
INITIALIZE DATA
HEADERS AND WRITE
INITIAL FIELDS

**CALL
RD_EKMAN_DATA**
READ IN PRE-
CALCULATED EKMAN
UPWELLING

START DAILY
LOOP

B

CALL TSBND
READ SURFACE
FORCING:
W STRESS, We,
AND HEAT FLUX

START HOURLY
LOOP

CALL SUN_INFO
COMPUTE
ZENITH ANGLE

**FUNCTION
FROUIN**
COMPUTE
TOTAL CLEAR
SKY RADIATION

CALL STRESS
CALL HFLUX
COMPUTE
SURFACE
STRESS AND
HEAT FLUX

COMPUTE
SOLAR
RADIATION THAT
PENETRATES
SURFACE

CALL PSTAR
COMPUTE NON-
DIMENSIONAL
ENTRAINMENT

CALL ENTR
COMPUTES ML
GROWTH AND
ADJUSTS
T(Z),S(z), & B(z)

CALL RETR
COMPUTES ML
RETREAT

CALL SHALLOW
LIMIT MINIMUM
MLD TO 101 CM

CALL RMODE
VERIFY THAT ML
RETREAT
CONSERVES B,T

CALL ABSRP1
ESTIMATE
TOTAL ENERGY
AFTER
ENTRAINMENT/
DETRAINMENT

**CALL
GREGG_CARDER**
COMPUTE PAR AT
EACH DEPTH

**CALL
WATERRAD**
COMPUTE
WATER COLUMN
RADIANCE

**CALL
BIOABSORB**
COMPUTE BIO
FEEDBACK

CALL EKMW
COMPUTE
EKMAN
UPWELLING

A

**Figure B1.1. Flowchart of ecosystem model coupled with the Garwood MLM.**

B.1.4 Routine Names and Functions

To better describe the functions of each FORTRAN module in the flowchart of Figure B1.1, a short explanation of each FORTRAN module is provided in Table B1.1. The list of modules in Table B1.1 is more extensive than the modules appearing in Figure B1.1 because some FORTRAN modules contain calls to subordinate FORTRAN routines and functions. The executable file for the ecosystem model is built by compiling and linking all relevant FORTRAN modules using a 'Makefile' provided with the source code package.

Table B1.1. Names and functionality of ecosystem model FORTRAN routines.

Routine Name	Description
ABSRP1	Absorption of radiation below the surface
ALGO	Contains: RIGHTHANDPZ,RIGHTHANDNN,PLEFTNEWPZ,PLEFTNEWNN,GAUSS
BSMN	Computes critical values of buoyancy to be used in entrainment calculation
BIOABSORB	Computes light absorption due to biology
ATMODD	Model of atmospheric transmittance of solar irradiance through marine atmosphere
COMP_ESTAR	Computes running daily mean of light at each depth (E^*)
COMPUTE_KV	Computes vertical eddy diffusivity coefficient for biological model equations
DAYTIM	Converts Gregorian to Julian, and Julian to Gregorian dates
DIFF	Computes vertical diffusion term (see also GARDIFF)
DIFFUSE	Name of FORTRAN file containing routine DIFF
EKMW	Estimates the Ekman upwelling profile given wind speed and latitude
ENERGY	Computes energy balance within the mixed layer
ENTR	Computes mixed-layer growth and adjusts profiles of temperature, salinity and buoyancy
FROUIN	Computes clear sky solar irradiance using Frouin et al. method
GAUSS	Gauss elimination implicit matrix solver for ecosystem model (Crank–Nicholson scheme)
GARDIFF	This routine is also part of the vertical diffusion computation
GREGG	Computes spectral solar irradiance using the Gregg and Carder method. Contains: GREGG_CARDER
GROWTH	Computes respiration and growth. Contains: GROWTH1,GROWTH2,RESIZ
HFLUX	Computes the surface heat flux
ICOND	Reads initial profiles of temperature and salinity
IMPMIX	Adjusts vertical profiles according to the depth change of the mixed layer
INITPZN	Initializes Phyto, Zoo, NH_4, and NO_3 concentrations
INIT	Initializes temperature and salinity fields
JPMIX	Relieves gradient Richardson number instability using J. Price's criterion
OPBLPC	Main program - Controls calls to all routines and main computational loop
OCEANSUB	Contains: WRITENITRATE,PROFHEADS,WTZPROFS,W_SERIES,W_SOLAR,WRITKT
LAST_TZ_SZ	Outputs temperature and salinity fields at last time step of computation
LEVMLD	Computes the mixed-layer depth
LIDATA	Opens and reads light data file
NAVAER	Computes aerosol parameters according to a simplified version of Navy model
NH4DOSE	Computes ammonium dosage for each daily interval
NH4OXTERM	Computes ammonium to nitrate conversion term
NH4RIGHT	Computes source and sink terms at the right hand side of the ammonium equation
NO3RIGHT	Computes source and sink terms at the right hand side of the nitrate equation
PLEFTNEWPZ	Assigns values to tridiagonal matrix that originate from P and Z equations
PLEFTNEWNN	Assigns values to tridiagonal matrix that originate from NH_4 and NO_3 equations
PRIGHT	Computes source and sink terms at the right hand side of the phytoplankton equation
PRIMARY	Computes gross, net and new production

PROFHEADS	Writes header information for the file containing the vertical profiles
PSTAR	Computes the non-dimensional entrainment
RD_EKMAN_DATA	Contains modules to read, calculate and manipulate Ekman pumping velocity
READPRF	Reads OGCM u, v, T, and w fields
RETR	Computes mixed-layer retreat (see RMODE)
RMODE	Computes ML retreat while conserving buoyancy, temp., salinity, and potential energy
RICH	Computes all biological quantities and forms right hand side of differential equations
RIGHTHANDNN	Computes diffusion and advection terms for the ammonium and nitrate equations
RIGHTHANDPZ	Computes diffusion and advection terms for the phytoplankton and zooplankton equations
SAVELAST	Save all biological variables at last time step for subsequent hot start of model
SFCRFL	Computes surface reflectance for direct and diffused components separately
SHALLOW	Limits minimum mixed-layer depth to a prescribed value (ex.: 101 cm)
SINKING	Computes sinking rate of phytoplankton
STATE	Computes buoyancy from temperature and salinity using simplified UNESCO equation
STRESS	Computes sea-surface wind stress
SUB	Contains: OPTICS,INITPZN,INIT1,INIT2,INIT3,PRIGHT,ZRIGHT,NH4RIGHT,NO3RIGHT,SINKING,PRIMARY,EKMW,COMPUTE_KV
SUN_INFO	Computes the solar zenith angle
TZ_SZ_USER	This routine is used in combination with ICOND
WATERRAD	Computes water column downwelling radiance
WRITENITRATE	Writes nitrogen production/loss to a file
WRITASC	Writes time series of bio-physical variables to a file
WRT_DIAG	Writes each term of the 4-component equations for diagnostic purposes
WTZPROFS	Writes daily time series of vertical profiles for selected model variables
ZRIGHT	Computes source and sink terms at the righthandside of the zooplankton equation

B.2 ECO1D with Chen et al. MLM Coupling or OGCM-driven Options

This section describes the input parameters, nominal values, input and output files, program flowchart, and FORTRAN routine names and functions for the ecosystem model using either the Chen et al. MLM or input from the OGCM.

B.2.1 Input Parameters and Nominal Values

As previously described in section B1.1, the input parameters and nominal values used by the ecosystem model are read in from a file (filename.par) specified in the command line when executing the model run:

% eco1d < filename.par &

The initial and forcing fields required for the multiyear runs are read in from other files specified in section B2.2. The format for all parameters in filename.par is provided in the include file 'reading.inc'. The following table summarizes each of the input parameters contained in the file.

IE=	Upwelling option: 0: use constant vertical velocity w_e 1: evoke Ekman upwelling calculation
CB=	Biological model option: 0: no biological model evoked 1: couple mixed layer model with biological model
IP=	Switch for initial nutrient concentration file: 1: use default values 2: read initial nitrate and ammonium concentrations from units 7,8 3: read initial nitrate and ammonium concentrations from hot start file (7) 4: read initial nitrate concentration from unit 7 and use default ammonium values
DD=	Switch to print results: 0: do not print results 1: print results
DB=	Switch to print daily-averaged time series of surface and depth-averaged values: 0: do not print time series 1: print time series
CV=	Switch to control writing of hot start file: 0: do not write hot start file 1: write hot start file
HR =	Controls frequency (in hours) of output of model variables (except for profiles)
HP =	Controls frequency (in hours) of output of vertical profiles
vapr= 2.79	Atmospheric water content (cm)
uo= 0.34	Ozone concentration (Dobson)
a_type=	Aerosol type: 0: Continental 1: Oceanic
Cldbb=0.50	Cloud correction coefficient

Cldaa=0.53   Cloud correction coefficient
dt=0.3600D+04   Model time step (seconds)
dz =0.1000D+01   Vertical grid resolution (meters)
Dep=250.0   Maximum depth for model calculations
AKD=0.0525   Coefficient for the vertical profile of diffusion for the bio model
ZONE=25.0   Depth of transition layer (meters)
BOTKV=8.65   Minimum vertical diffusivity Kv (m^2/d)
We= 0.3   Upwelling velocity (m/d)
LAT= 0.0   Latitude in degrees (North is positive)
LON= 165.0   Longitude in degrees (East is positive)

IW=   Control for upwelling velocity:
                               1: constant We
                               2: read in We from external source

m= 0.1   Phytoplankton death rate, d^{-1}
G0= .8511   Phytoplankton growth rate at $0^{\circ}C$, d^{-1}
Kno3= 1.0000   Half saturation of nitrate uptake, mg-at N m^{-3}
Knh4= .5000   Half saturation of ammonium uptake, mg-at N m^{-3}
c= 0.02   Ratio of phytoplankton respiration to growth
Agk= .0633   Temperature sensitivity of algal growth, $1/^{\circ}C$
Ark= .0633   Temperature sensitivity of algal respiration, $1/^{\circ}C$
Ideep = 400.0   Maximum photoacclimation parameter ($\geq$ 60 m), μmol quanta/m^2/s
Ishal= 400.0   Maximum photoacclimation parameter (< 60 m), μmol quanta/m^2/s
mixed= 60.0   Critical depth (meters) for Ishal and Ideep calculation
NH4= 0.1   Default initial NH4 value (if input file not assigned)
NO3= 23.0   Default initial NO3 value (if input file not assigned)
P = .1000   Initial Phytoplankton concentration, mg-at N m^{-3}
Z = .1000   Initial Zooplankton concentration, mg-at N m^{-3}
pk= 5.0   Nitrate-sensitive coefficient due to ammonium
Knir= 2.5   Attenuation coefficient for Near Infrared (m^{-1})
K_v = 1.0   Minimum value for K_v (m^2/d)
CHLN= 1.0   Chlorophyll-a:Nitrogen ratio, mg/mg-at N
DI = 4   Index to control the method to compute surface diffusivity
cs= 2   Index for choosing the method to compute the diffusivity profile
fc=1.0   Multiplicative factor to apply to vertical diffusivity
Smax= 0.0   Sinking speed (m/d)
g= 0.04   Zooplankton death rate, d^{-1}
Rm= 7.0   Zooplankton maximum grazing rate, d^{-1}
LAMBDA= 0.8   Ivlev constant, m^3/mg-at N
GAMMA= 0.3   Unassimilated zooplankton ingested ratio
rz0= 0.019   Not used - reformulated
krz= 0.08   Temperature sensitivity of zooplankton respiration, $1/^{\circ}C$
az = 0.6   Fraction of dead zooplankton converted to ammonium
ap = 0.6   Fraction of dead phytoplankton converted to ammonium
TH = 0.0   Minimum C threshold for zooplankton grazing, mgC/m^3
MOVING= 24   Moving average window in hours for light energy
START= 19830701   Starting date for calculations, year/month/day
NDAYS=365   Total number of days of simulation

IMLD= 1   Switch for depth integration limits (T1)
                               1: surface to mixed-layer depth

2: surface to bottom

T2= 50.0	Integration depth limits
T3= 250.0	Integration depth limits
DLEVEL= 250.0	Maximum depth level for model output
INTV= 10.0	Depth interval for output
Anmax= 02.00	Maximum rate of nitrification, nmol/day
Dmin= .0095	Minimum irradiance (300 - 470 nm) for nitrification, W/m^2
KD = 0.0360	Half-saturation dosage for nitrification photoinhibition, $W/m^2/nm$
Cpel =0.80	Remineralization coefficient for fecal pellets
CN =0.1	Dissipation coefficient of Equation 1.2
CM =0.85	Dissipation coefficient of Equation 1.2
GAMA=0.23	Coefficient for partial solar radiation (PAR 280 - 700 nm)
TAUMN=0.00005	Minimum value of wind stress
KVALE=0.0	Coefficient of flux adjustment
HP= 20.0	Attenuation depth for shortwave radiation
Hmin=5.0	Minimum mixed layer depth (meters)
Hmax=150.0	Maximum mixed layer depth (meters)
WPC=10.0	wp*wpc
EP=0.00001	epsilon
KTB=0.0	Background mixing coefficient for temperature and salinity (m^2/s)
KVB=0.0	Background mixing coefficient for u and v (m^2/s)
RIC1=0.65	Parameter for const. Richardson No. profile (instability adjust., J. Price, WHOI)
RIC2=0.25	Parameter for constant Richardson number profile (after J. Price, WHOI)
GAM1=0.4	Parameter for constant Richardson number profile (after J. Price, WHOI)
GAM2=0.4	Parameter for constant Richardson number profile (after J. Price, WHOI)
IHP=0	Switch for attenuation depth scheme
	0: calculate attenuation depth from light profile
	1: use constant value of 17 meters
COUPLED = 0	Control index in main module to couple (1)/uncouple(0) bio turbidity in water with light absorption coefficient
UPWEL=1	Control index to include(1)/exclude(0) upwelling in computation

B.2.2 Input and Output files

The following logic units (LU) and input/output file names are specified in 'filename.par' after the last parameter input described in section B2.1. The file names and data sets that they contain are only given as examples; other data sets for different time periods and geographical areas can be specified by the user. Note that LU=TMP means temporary logic unit.

Logic units (LU) for input/output files

1 2 3 11 12 13 14 7 8 9 80 90

Input files

/user_pathname/xbt250.dat	LU=01;	Initial temperature profiles from XBTs
/user_pathname/testmet8792.dat	LU=02;	Environmental data from TOGA/TAO (1987–1992)
/user_pathname/raguw8792.dat	LU=03;	OGCM vertical velocities (1987–1992)

Output Files

/user_pathname/namef.asc	LU=11:	Daily time series of selected diagnostic and predicted model variables (see Table A6)
/user_pathname/namep.asc	LU=12:	Daily time series of vertical profiles for selected model variables (see Table A7)
/user_pathname/namet.asc	LU=13:	Daily time series of column-averaged and surface values for selected model variables (see Table A8)
/user_pathname/namen.asc	LU=14:	More daily time series of selected diagnostic and predicted model variables (see Table A9)
/user_pathname/diag_bal_name.dat	LU=88:	Diagnostic file containing daily profiles of all equation terms (Phyto, Zoo, NO_3 and NH_4)

Input files

/user_pathname/nitr165e.dat	LU=07:	Climatological nitrate (NO_3) concentration profile
/user_pathname/winnh4.dat	LU=08:	Climatological ammonium (NH_4) concentration profile

Output Files

/user_pathname/lastdyn.bin	LU=TMP:	Binary file containing dynamic variables from last time step to be used for hot starting the model
/user_pathname/lastbio.bin	LU=TMP:	Binary file containing biological variables from last time step to be used for hot starting the model

Input files

/user_pathname/uvatmodd.dat	LU=TMP:	Spectral absorption coefficients for Gregg-Carder model
/user_pathname/wv_chl_absp.dat	LU=TMP:	Attenuation coefficients due to chlorophyll
/user_pathname/asnh4.dat	LU=TMP:	Ammonium nitrification coefficients
/user_pathname/testrad8792.dat	LU=TMP:	Radiation data from TOGA–TAO (1987–1992)
/user_pathname/uvtw83792n.dat	LU=09:	Time series of u, v, w and temp from OGCM
/user_pathname/uvtc83792.day	LU=80:	Monthly atmospheric u, v, T,cloud fraction data from ISCCP
/user_pathname/mixed83792.dat	LU=90:	Mixed layer depth time series (19983–1992) from OGCM

B.2.4 Ecosystem Model Flowchart

Figure B2.1 shows a flowchart of the second and third versions of the ecosystem model which features options for a stand-alone calculation of the temperature and vertical diffusivity profiles using the Chen et al. [1994] mixed-layer model, and one-way coupling of velocity and temperature fields derived from the

OGCM. The flowchart identifies each main FORTRAN module in a separate box, with the arrows indicating input/output data flows and time stepping loops.
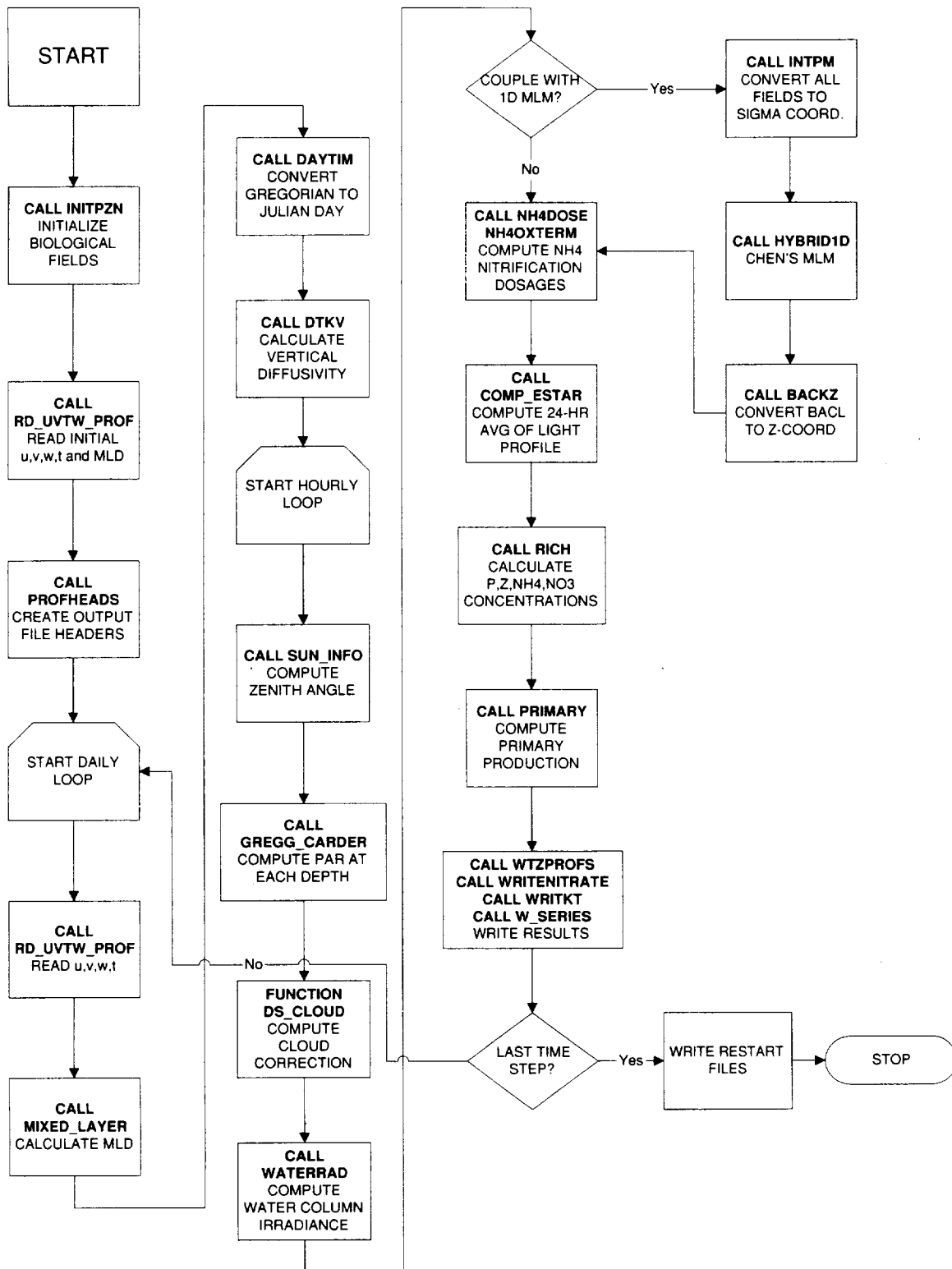
Figure B2.1. Flowchart of ecosystem model with one-way coupling to OGCM physical parameters. Note that there is an option to couple the biology with the Chen MLM.

B.2.5 Routine Names and Functions

To better describe the functions of each FORTRAN module in the flowchart of Figure B2.1, a short explanation of each FORTRAN module is provided in Table B2.1. The list of modules in Table B2.1 is more extensive than the modules appearing in Figure B2.1 because some FORTRAN modules contain calls to subordinate FORTRAN routines and functions. The executable file for the ecosystem model is built by compiling and linking all relevant FORTRAN modules using a 'Makefile' provided with the source code package.

Table B2.1. Names and functionality of ecosystem model FORTRAN routines.

Routine Name	Description
ABSPAR	Contains WATERRAD - Computes water column irradiance
ALGO	Contains: RIGHTHANDPZ,RIGHTHANDNN,PLEFTNEWPZ,PLEFTNEWNN,PLEFT,GAUSS
ATMODD	Model of atmospheric transmittance of solar irradiance through marine atmosphere
BACKZ	Converts σ coordinate to z coordinate
COMP_ESTAR	Computes running daily mean of light at each depth (E^*)
CVMIX	Convective adjustment of T, S, B, U, and V fields for the Chen mixed-layer model
DAYTIM	Converts Gregorian to Julian, and Julian to Gregorian dates
DCHEN	This module contains routines for the Chen mixed-layer model
DENS	Computes seawater density from temperature, salinity and pressure
DIFFUSION	Contains mixing and advection modules (BKMIXINGW,BKMIXING,ADVECTION) for Chen's MLM
ENERGY	Computes energy balance within the mixed layer
FROUIN	Computes clear sky solar irradiance using Frouin et al. method
GAUSS	Gauss elimination implicit matrix solver for ecosystem model (Crank–Nicholson scheme)
GREGG	Computes spectral solar irradiance using the Gregg and Carder method. Contains: GREGG_CARDER
GROWTH	Computes respiration and growth. Contains: GROWTH1,GROWTH2,RESIZ
HYBRID1D	Chen's 1D MLM using hybrid vertical mixing scheme
IMPMIX	Adjusts vertical profiles according to the depth change of the mixed layer
INIT	Initializes temperature and salinity fields
INTERPRF	Reads u, v, T OGCM profiles at 10-m intervals, interpolates values onto a 1-m spacing, calculates the Richardson number and mixed-layer depth. Contains: RD_UVTW_PROF,INTERPOL,DVARDZ,RICHARDSON,MIXED_LAYER,REALFT
INITPZN	Initializes the phytoplankton, zooplankton, ammonium and nitrate fields
JPMIX	Relieves gradient Richardson number instability using J. Price's criterion
KTMIX	Calculates vertical mixing using the Kraus–Turner scheme
KTMODEL	Main program - reads/writes data and controls calls to all routines and main computational loop
KTMSUB	Contains: WRITENITRATE,PROFHEADS,WTZPROFS,W_SERIES,W_SOLAR,WRITKT
LAST_TZ_SZ	Outputs temperature and salinity fields at last time step of computation
LIDATA	Opens and reads light data file
NAVAER	Computes aerosol parameters according to a simplified version of Navy model
NH4DOSE	Computes Ammonium dosage for each daily interval
NH4OXTERM	Computes ammonium to nitrate conversion term
NH4RIGHT	Computes source and sink terms at the right hand side of the ammonium equation
NO3RIGHT	Computes source and sink terms at the right hand side of the nitrate equation
PLEFTNEWPZ	Assigns values to tridiagonal matrix that originate from P and Z equations
PLEFTNEWNN	Assigns values to tridiagonal matrix that originate from NH_4 and NO_3 equations
PRIGHT	Computes source and sink terms at the right hand side of the phytoplankton equation
PRIMARY	Computes gross, net and new production

PROFHEADS	Writes the header for the file containing the time series of vertical profiles
RD_EKMAN_DATA	Contains modules to read, calculate and manipulate Ekman pumping velocity
READPRF	Reads OGCM u, v, T, and w fields
RICH	Computes all biological quantities and forms right hand side of differential equations
RIGHTHANDNN	Computes diffusion and advection terms for the ammonium and nitrate equations
RIGHTHANDPZ	Computes diffusion and advection terms for the phytoplankton and zooplankton equations
RICHARDSON	Computes the vertical mixing coefficient (K_v) using the Pacanowski and Philander scheme
SAVELAST	Save all biological variables at last time step for subsequent hot start of model
SFCRFL	Computes surface reflectance for direct and diffused components separately
STATE	Computes buoyancy from temperature and salinity using simplified UNESCO equation
SUB	Contains: OPTICS,INITPZN,INIT1,INIT2,INIT3,PRIGHT,ZRIGHT,NH4RIGHT,NO3RIGHT,SINKING,PRIMARY,EKMW,COMPUTE_KV,DTKV,DTKV8,KD_PROFILE, KVISINSIGMA
SUNINFO	Computes the solar zenith angle
TKE0	Computes total turbulent kinetic energy to be used in Chen's MLM
TRIDIAG	Tridiagonal matrix solver for the implicit Crank–Nicholson finite difference method
WRITENITRATE	Writes nitrogen production/loss to a file
.WTZPROFS	Writes the daily time series of profiles to unit 12
W_SERIES	Writes the daily time series of surface and vertically averaged variables to unit 13
WRT_DIAG	Writes each term of the 4-component equations for diagnostic purposes
ZRIGHT	Computes source and sink terms at the righthandside of the zooplankton equation

REFERENCES

Austin , R. W., 1974: The remote sensing of spectral radiance from below the ocean surface. In: *Optical Aspects of Oceanography*, edited by N. G. Jerlov and E. Steeman Nielsen, Academic, San Diego, Calif., 317–344.

Baker, K. S., and R. C. Smith, 1982: Bio-optical classification and model of natural waters, 2. *Limnol. Oceanogr.*, **27**, 500–509.

Berliand, M. E., and T. G. Berliand, 1952: Determining the net long-wave radiation of the Earth with consideration of the effect of cloudiness. *Izv. Akad. Nauk. SSSR Ser. Geofiz., 1*.

Bishop, J. K. B., and W. B. Rossow, 1991: Spatial and temporal variability of global surface solar irradiance. *J. Geophys. Res.*, **96(C9)**, 16,839–16,858.

Blanchot, J., M. Rodier and A. Le Bouteiller, 1992: Effect of El Niño southern oscillation events on the distribution of phytoplankton in the Western Pacific tropical ocean. *J. Plankton Res.*, **14**, 137–156.

Brock, J. C., C. R. McClain, M. E. Luther and W. W. Hay, 1991: The phytoplankton bloom in the northwest Arabian Sea during the southwest monsoon of 1979. *J. Geophys. Res.*, **96**, 20,623–20,642.

Budyko, M. I., 1974: *Climate and Life*, 508 pp., Academic, San Diego, Calif.

Chavez, F. P., K. R. Buck, K. H. Coale, J. H. Martin, G. R. DiTullio, N. A. Welschmeyer, A. C. Jacobson and R. T. Barber, 1991: Growth rates, grazing, sinking, and iron limitation of equatorial Pacific phytoplankton. *Limnol. Oceanogr.*, **36**, 1816–1831.

Chen, D., A. Busalacchi, and L. Rothstein, 1994: The roles of vertical mixing, solar radiation, and wind stress in a model simulation of the sea surface temperature seasonal cycle in the tropical Pacific Ocean. *J. Geophys. Res.*, **99**, 20,345–20,359.

Conkright, M., S. Levitus and T. Boyer, 1994: NOAA Atlas NESDIS 1, World Ocean Atlas 1994, Vol. 1, Nutrients. U.S. Department of Commerce, 150 pp.

Cronin, M., and M. J. McPhaden, 1997: The upper ocean heat balance in the western equatorial Pacific warm pool during September–December 1992. *J. Geophys. Res.*, **102**, 8,533–8553.

Dam, H. G., X. Zhang, M. Butler and M. R. Roman, 1995: Mesozooplankton grazing and metabolism at the equator in the central Pacific, Part II: Implications for carbon and nitrogen fluxes. *Deep Sea Res.*, **42**, 735–756.

Darzi, M., J. K. Firestone, G. Fu, E. Yeh and C. R. McClain, 1991: Current efforts regarding the SEAPAK oceanographic analysis software system, *Proc. Seventh Int. Conf. Interactive and Processing Systems for Meteorol., Oceanogr., and Hydrol.*, Am. Meteorol. Soc., New Orleans, Jan. 14-18, 109–115.

Delcroix, T., and C. Henin, 1991: Seasonal and interannual variations of sea-surface salinity in the tropical Pacific Ocean. *J. Geophys. Res.*, **96**, 22,135–22,150.

Delcroix, T., G. Eldin, M. H. Radenac, J. Toole and E. Firing, 1992: Variations of the western equatorial Pacific Ocean, 1986–1988. *J. Geophys. Res.*, **97**, 5423–5447.

Delcroix, T., G. Eldin, M. McPhaden and A. Moliere, 1993: Effects of westerly wind bursts upon the western equatorial Pacific Ocean, February–April 1991. *J. Geophys. Res.*, **98**, 16,379–16,385.

Denman, K. L., and M. Miyake, 1973: Upper layer modification at Ocean Station *Papa*: Observations and simulation. *J. Phys. Oceanogr.*,**3**, 185–196.

Dobson, F. W., and S. D. Smith, 1988: Bulk models of solar radiation at sea. *Q. J. R. Meteorol. Soc.*, **114**, 165–182.

Eppley, R. W., 1972: Temperature and phytoplankton growth in the sea. *Fish. Bull.*, **70**, 1063–1085.

Firestone, J., G. Fu, J. Chen, M. Darzi and C. McClain, 1989: PC-SEAPAK software for oceanographic data analysis; An update. *Proc. Fifth Int. Conf. Interactive and Inform. Processing Systems for Meteorol., Oceanogr., and Hydrol.*, Am. Meteorol. Soc., Anaheim Jan. 29-Feb. 3, 33–39.

Firestone, J., G. Fu, M. Darzi and C. McClain, 1990: NASA's-SEAPAK software for oceanographic data analysis; An update. *Proc. Sixth Int. Conf. Interactive and Inform. Processing Systems for Meteorol., Oceanogr., and Hydrol.*, Am. Meteorol. Soc., Anaheim Feb. 5-9, 260–267.

Frost, B. W., 1991: The role of grazing in nutrient-rich areas of the open ocean. *Limnol. Oceanogr.*, **36**, 1616–1630.

Frost, B. W., 1993: A modeling study of the processes regulating plankton standing stock and production in the open subarctic Pacific Ocean. *Prog. Oceanogr.*, **32**, 101–135.

Frouin, R., D .W. Lingner, C. Gautier, K. S. Baker and R. C. Smith, 1989: A simple analytical formula to compute clear sky total and photosynthetically available solar irradiance at the ocean surface. *J. Geophys. Res.*, **94(C7)**, 9731–9742.

Furuya, K., 1990: Subsurface chlorophyll maximum in the tropical and subtropical western Pacific Ocean: vertical profiles of phytoplankton biomass and its relationship with chlorophyll-*a* and particulate organic carbon. *Mar. Biol.*, **107**, 529–539.

Garwood, R. W., 1977: An oceanic mixed-layer model capable of simulating cyclic states. *J. Phys. Oceanogr.*, **7**, 455–471.

Gent, P., and M. A, Cane, 1989: A reduced gravity, primitive equation model of the upper equatorial ocean. *J. Comput. Phys.*, **81**, 444–480.

Gregg, W. W., and K. L. Carder, 1990: A simple spectral solar irradiance model for cloudless marine atmosphere. *Limnol. Oceanogr.*, **35(8)**, 1657–1675.

Huang, R. X., 1993: Real freshwater flux as natural boundary condition for salinity balance and thermohaline circulation forced by evaporation and precipitation. *J. Phys. Oceanogr.*, **23**, 2428–2446.

Ikeda, T., 1985: Metabolic rates of epipelagic marine zooplankton as a function of body mass and temperature. *Mar. Biol.*, **85**, 1–11.

Karl, D. M., and A. F. Michaels, eds., 1996: Ocean time-series: Results from the Hawaii and Bermuda research programs. *Deep Sea Res. Part II*, **43** (2-3), 683 pp.

Koepke, P., 1984: Effective reflectance of oceanic whitecaps. *Appl. Opt.*, **23**, 1816–1824.

Large, W. G., J. C. McWilliams, and S. C. Doney, 1994: Oceanic vertical mixing: A review and a model with a nonlocal boundary layer parameterization. *Rev. Geophys.*, **32**, 363–403.

Le Borgne, R. and M. Rodier, 1996: Net zooplankton and the biological pump, Part II: A comparison between the oligotrophic and mesotrophic equatorial Pacific. *Deep Sea Res.*, submitted.

Leonard, C. L., and C. R. McClain, 1998: An iron-based ecosystem model of the central equatorial Pacific. *J. Geophys. Res.*, submitted.

Lewis, M. R., M. -E. Carr, G. C. Feldman, W. E. Esaias and C. R. McClain, 1990: Satellite estimates of the influence of penetrating solar radiation on the heat budget of the equatorial Pacific Ocean. *Nature*, **347**, 543–545.

Lukas, R., and E. Lindstrom, 1991: The mixed layer of the western equatorial Pacific. *J. Geophys. Res.*, **96**, 3,343–3,357.

Martin, P. J., 1985: Simulation of the mixed layer at OWS November and Papa with several models. *J. Geophys. Res.*, **90**, 903–916.

McClain, C. R., W. E. Esaias, G. C. Feldman, J. Elrod, D. Endres, J. Firestone, M. Darzi, R. Evans and J. Brown, 1990: Physical and biological processes in the North Atlantic during the First Global GARP Experiment. *J. Geophys. Res.*, **95**, 18,027–18,048.

McClain, C. R., G. Fu, M. Darzi, and J. K. Firestone, 1992: PC-SEAPAK User's Guide, Version 4.0. *NASA Tech. Mem.*, **104557**.

McClain, C. R. and J. K. Firestone, 1993: An investigation of Ekman upwelling in the North Atlantic. *J. Geophys. Res.*, **98**, 12,237–12,339.

McClain, C. R., K.-S. Tai and D. Turk, 1996: Observations and simulations of physical and biological processes at ocean weather station P, 1951-1980. *J. Geophys. Res.*, **101**, 3697–3713.

McClain, C. R., R. Murtugudde, S. R. Signorini, and K. S. Tai, 1998: A simulation of biological processes in the equatorial Pacific warm pool at 165°E. *J. Geophys. Res.*, (submitted).

McPhaden, M., and S. Hayes, 1991: On the variability of winds, sea surface temperature, and surface layer heat content in the western equatorial Pacific. *J. Geophys. Res.*, **96**, 3,331–3,342.

Mellor, G. L., 1991: An equation of state for numerical models of oceans and estuaries. *J. Atmos. Oceanic Technol.*, **8**, 609–611.

Monahan, E. C., and I. O'Muircheartaigh, 1980: Optical power-law description of oceanic whitecap coverage dependence on wind speed. *J. Phys. Oceanogr.*, **10**, 2094–2099.

Monod, J., 1942: Recherches sur la croissance de cultures bacteriennes. Hermann, Paris.

Morel, A., and L. Prieur, 1977: Analysis of variations in ocean color. *Limnol. Oceanogr.*, **22**, 709–722.

Morel, A., 1988: Optical modeling of the upper ocean in relation to its biogenous matter content (case I waters). *J. Geophys. Res.*, **93**, 10,749–10,768.

Mueller, J. L., and R. E. Lang, 1989: Bio-optical provinces of the northeast Pacific Ocean: A provisional analysis. *Limnol. Oceanogr.*, **34**, 1,572–1,586.

Murtugudde, R., M. Cane, and V. Prasad, 1995: A reduced gravity, primitive equation, isopycnal ocean GCM: Formulation and simulations. *Mon. Wea. Rev.*, **123**, 2864–2887.

Murtugudde, R., R. Seager and A. Busalacchi, 1996: Simulation of the tropical oceans with an ocean GCM coupled to an atmospheric mixed layer model. *J. Climate*, **9**, 1795–1815.

Murtugudde, R., and A. Busalacchi, 1998: Salinity effects in a tropical ocean model. *J. Geophys. Res.*, **103**, 3283–3300.

Neuberger, H., 1951: *Introduction to Physical Meteorology*. Pennsylvania State University, University Park, 271pp.

Ocean Studies Board, 1994: The ocean's role in global change, 85 pp., *Natl. Acad. Press*, Washington, D. C.

Olsen, L. M. and C. McClain, 1992: Cooperative efforts in support of ocean research through NASA's Climate Data System. *Proc. Eigth Int. Conf. Interactive and Inform. Processing Systems for Meteorol., Oceanogr., and Hydrol.*, Am. Meteorol. Soc., Atlanta, Jan. 5-10, 206–211.

Olson, R. J., 1981: Differential photoinhibition of marine nitrifying bacteria: A possible mechanism for the formation of the primary nitrate maximum. *J. Mar. Res.*, **39**, 227–238.

Pacanowski, R. C., and G. H. Philander, 1981: Parameterization of vertical mixing in numerical models of tropical oceans. *J. Phys. Oceanogr.*, **11**, 1443–1451.

Press, W. H., B. P. Flannery, S. A. Teukolsky, and W. T. Vetterling, 1988: *Numerical Recipies in C, The Art of Scientific Computing*, Cambridge Univ. Press., New York, 735 pp.

Price, J. R., R. Weller and R. Pinkel, 1986: Diurnal cycle – Observations and models of the upper the upper ocean response to diurnal heating, cooling, and winter mixing. *J. Geophys. Res.*, **91**, 8411–8427.

Reed, R. K., 1977: An estimate of the climatological heat fluxes over the tropical Pacific ocean. *J. Clim. Appl. Meteorol.*, **24**, 833–840.

Reinecker, M. M., and L. L. Ehret, 1988: Wind stress curl variability over the North Pacific from the Comprehensive Ocean-Atmosphere Data Set. *J. Geophys. Res.*, **93**, 5069–5077.

Schiffer, R. A., and W. B. Rossow, 1985: ISCCP global radiance data set – a new resource for climate research. *Bull. Am. Meteorol. Soc.*, **66**(12), 1498–1505.

Siegel, D. A., J. C. Ohlmann, L. Washburn, R. R. Bidigare, C. Nosse, E. Fields, and Y. Zhou, 1995: Solar radiation, phytoplankton pigments and radiant heating of the equatorial Pacific warm pool. *J. Geophys. Res.*, **100**, 4885–4891.

Smith, W. L., 1966: Note on the relationship between total precipitable water and surface dew point. *J. Appl. Meteorol.*, **5**, 726–727.

Subcommittee on Global Change Research, 1995: *Our Changing Planet, The FY 1995 U. S. Global Change Research Program*, 132 pp., Off. Of Sci. and Technol. Policy, Washington, D. C.

Tai, K.-S., and C. R. McClain, 1993: Recent enhancements of IDAPAK, a PC-based interactive data analysis package. Paper presented at the Ninth International Conference on Interactive Information and Processing Systems for Meteorology, Oceanography, and Hydrology. *Am. Meteorol. Soc.*, Anaheim, Calif., Jan. 17–22, 1993.

Tai, K.-S., and C. R. McClain, 1996: IDAPAK, interactive analysis of oceanographic and meteorological data for UNIX workstations. Proceedings of the Twelfth International Conference on Interactive Information and Processing Systems for Meteorology, Oceanography, and Hydrology. *Am. Meteorol. Soc.*, Atlanta, GA, Jan. 28–Feb. 2, 1996, 533–538.

Tetens, O., 1930: Übereinige meteorologische Begriffe. *Z. Geophys.*, 6, 297–309.

Wang, W., and M. J. McPhaden, 1998: The surface layer heat balance in the equatorial Pacific Ocean, Part I: Mean seasonal cycle. *J. Phys. Oceanogr.*, (submitted).

Webster, P. J., and R. Lukas, 1992: TOGA-COARE: The Coupled Ocean-Atmosphere Response Experiment. *Bull. Am. Meteorol. Soc.*, 73, 1377–1416.

Woodruff, S. D., R. J. Slutz, R. L. Jenne, and P. M. Steurer, 1987: A comprehensive ocean-atmosphere data set. *Bull. Am. Meteorol. Soc.*, 68, 1239–1250.

Wroblewski, J. S., 1977: A model of phytoplankton plume formation during variable Oregon upwelling. *J. Mar. Res.*, 35, 357–394.

Wroblewski, J. S. and R. G. Richman, 1987: The non-linear response of plankton to wind mixing events – Implications for survival of larval northern anchovy. *J. Plankton Res.*, 9, 103–123.

Xie, P., and P. Arkin, 1996: An intercomparison of gauge observations and satellite estimates of monthly precipitation. *J. Appl. Meteorol.*, 34, 1143–1160.

Zeebe, R. E., H. Eicken, D. H. Robinson, D. Wolf-Gladrow, and G. S. Dieckmann, 1996: Modeling the heating and melting of sea ice through light absorption by microalgae. *J. Geophys. Res.*, 101, 1163–1181.

REPORT DOCUMENTATION PAGE

Public reporting burden for this collection of information is estimated to average 1 hour per response, including the time for reviewing instructions, searching existing data sources, gathering and maintaining the data needed, and completing and reviewing the collection of information. Send comments regarding this burden estimate or any other aspect of this collection of information, including suggestions for reducing this burden, to Washington Headquarters Services, Directorate for Information Operations and Reports, 1215 Jefferson Davis Highway, Suite 1204, Arlington, VA 22202-4302, and to the Office of Management and Budget, Paperwork Reduction Project (0704-0188), Washington, DC 20503.

1. AGENCY USE ONLY *(Leave blank)*	2. REPORT DATE April 1998	3. REPORT TYPE AND DATES COVERED Technical Memorandum

4. TITLE AND SUBTITLE

An Ecosystem Model for Simulation of Physical and Biological Oceanic Processes—IDAPAK User's Guide and Applications

5. FUNDING NUMBERS

Code 970.2

6. AUTHOR(S)

Charles R. McClain, Sergio R. Signorini, King-Sheng Tai, Kevin Arrigo, and Ragu Murtugudde

7. PERFORMING ORGANIZATION NAME(S) AND ADDRESS (ES)

Laboratory for Hydrospheric Processes
Goddard Space Flight Center
Greenbelt, Maryland 20771

8. PEFORMING ORGANIZATION REPORT NUMBER

98B00042

9. SPONSORING / MONITORING AGENCY NAME(S) AND ADDRESS (ES)

National Aeronautics and Space Administration
Washington, DC 20546-0001

10. SPONSORING / MONITORING AGENCY REPORT NUMBER

NASA/TM–1998–206856

11. SUPPLEMENTARY NOTES

Charles R. McClain and Kevin Arrigo: NASA Goddard Space Flight Center, Greenbelt, Maryland
Sergio Signorini and King-Sheng Tai: SAIC General Sciences Corporation, Laurel, Maryland
Ragu Murtugudde: University of Maryland, College Park, Maryland

12a. DISTRIBUTION / AVAILABILITY STATEMENT

Unclassified–Unlimited
Subject Category: 48
Report available from the NASA Center for AeroSpace Information,
7121 Standard Drive, Hanover, MD 21076-1320. (301) 621-0390.

12b. DISTRIBUTION CODE

13. ABSTRACT *(Maximum 200 words)*

This TM describes the development, testing, and application of a 4-component (phytoplankton, zooplankton, nitrate, and ammonium) ecosystem model capable of simulating oceanic biological processes. It also reports and documents an in-house software package (Interactive Data Analysis Package - IDAPAK) for interactive data analysis of geophysical fields, including those related to the forcing, verification, and analysis of the ecosystem model. Two regions were studied in the Pacific: the Warm Pool (WP) in the Equatorial Pacific (165°E at the equator) and at Ocean Weather Station P (OWS P) in the Northeast Pacific (50°N, 145°W).

The WP results clearly indicate that the upwelling at 100 meters correlates well with surface blooms. The upwelling events in late 1987 and 1990 produced dramatic increases in the surface layer values of all 4 ecosystem components, whereas the spring-summer deep mixing events, do not seem to incur a significant response in any of the ecosystem quantities.

The OWS P results show that the monthly profiles of temperature, the annual cycles of solar irradiance, and 0- to 50-m integrated nitrate accurately reproduce observed values. Annual primary production is 190 gC/m²/yr, which is consistent with recent observations but is much greater than earlier estimates.

14. SUBJECT TERMS

Ecosystem modeling, tropical Pacific, north Pacific, interactive data analysis software.

15. NUMBER OF PAGES
67

16. PRICE CODE

17. SECURITY CLASSIFICATION OF REPORT Unclassified	18. SECURITY CLASSIFICATION OF THIS PAGE Unclassified	19. SECURITY CLASSIFICATION OF ABSTRACT Unclassified	20. LIMITATION OF ABSTRACT UL